

Review Article

The Era of Kilometer-Scale Neutrino Detectors

Francis Halzen¹ and Uli Katz²

¹ *Wisconsin IceCube Particle Astrophysics Center, University of Wisconsin-Madison, Madison, WI 53706, USA*

² *Erlangen Centre for Astroparticle Physics (ECAP), University of Erlangen-Nuremberg, 91058 Erlangen, Germany*

Correspondence should be addressed to Francis Halzen; halzen@icecube.wisc.edu

Received 18 July 2012; Accepted 18 October 2012

Academic Editor: Jose Bernabeu

Copyright © 2013 F. Halzen and U. Katz. This is an open access article distributed under the Creative Commons Attribution License, which permits unrestricted use, distribution, and reproduction in any medium, provided the original work is properly cited.

Neutrino astronomy beyond the Sun was first imagined in the late 1950s; by the 1970s, it was realized that kilometer-scale neutrino detectors were required. The first such instrument, IceCube, transforms a cubic kilometer of deep and ultra-transparent Antarctic ice into a particle detector. KM3NeT, an instrument that aims to exploit several cubic kilometers of the deep Mediterranean sea as its detector medium, is in its final design stages. The scientific missions of these instruments include searching for sources of cosmic rays and for dark matter, observing Galactic supernova explosions, and studying the neutrinos themselves. Identifying the accelerators that produce Galactic and extragalactic cosmic rays has been a priority mission of several generations of high-energy gamma-ray and neutrino telescopes; success has been elusive so far. Detecting the gamma-ray and neutrino fluxes associated with cosmic rays reaches a new watershed with the completion of IceCube, the first neutrino detector with sensitivity to the anticipated fluxes. In this paper, we will first revisit the rationale for constructing kilometer-scale neutrino detectors. We will subsequently recall the methods for determining the arrival direction, energy and flavor of neutrinos, and will subsequently describe the architecture of the IceCube and KM3NeT detectors.

1. Introduction

Soon after the 1956 observation of the neutrino [1], the idea emerged that it represented the ideal astronomical messenger. Neutrinos travel from the edge of the Universe essentially without absorption and with no deflection by magnetic fields. Having essentially no mass and no electric charge, the neutrino is similar to the photon, except for one important attribute: its interactions with matter are extremely feeble. So, high-energy neutrinos may reach us unscathed from cosmic distances, from the inner neighborhood of black holes, and, hopefully, from the nuclear furnaces where cosmic rays are born. Their weak interactions also make cosmic neutrinos very difficult to detect. Immense particle detectors are required to collect cosmic neutrinos in statistically significant numbers [2]. By the 1970s, it was clear that a cubic-kilometer detector was needed to observe cosmic neutrinos produced in the interactions of cosmic rays with background microwave photons [3]. Newer estimates for observing potential cosmic accelerators such as Galactic supernova remnants and

gamma-ray bursts unfortunately point to the same exigent requirement [4–6]. Building a neutrino telescope has been a daunting technical challenge.

Given detector's required size, early efforts concentrated on transforming large volumes of natural water into Cherenkov detectors that catch the light produced when neutrinos interact with nuclei in or near the detector [7]. After a two-decade-long effort, building the Deep Underwater Muon and Neutrino Detector (DUMAND) in the sea off the main island of Hawaii unfortunately failed [8]. However, DUMAND paved the way for later efforts by pioneering many of the detector technologies in use today and by inspiring the deployment of a smaller instrument in Lake Baikal [9], as well as efforts to commission neutrino telescopes in the Mediterranean [10–12]. These have paved the way towards the construction of KM3NeT. The first telescope on the scale envisaged by the DUMAND collaboration was realized instead by transforming a large volume of the extremely transparent natural deep Antarctic ice into a particle detector, the Antarctic Muon and Neutrino Detector Array

(AMANDA). In operation since 2000, it represents a proof of concept for the kilometer-scale neutrino observatory, IceCube [13, 14].

Neutrino astronomy has already achieved spectacular successes: neutrino detectors have “seen” the Sun and detected a supernova in the Large Magellanic Cloud in 1987. Both observations were of tremendous importance; the former showed that neutrinos have a tiny mass, opening the first crack in the standard model of particle physics, and the latter confirmed the basic nuclear physics of the death of stars. Figure 1 illustrates the cosmic neutrino energy spectrum covering an enormous range, from microwave energies 10^{-12} eV to 10^{20} eV [15]. The figure is a mixture of observations and theoretical predictions. At low energy, the neutrino sky is dominated by neutrinos produced in the Big Bang. At MeV energy, neutrinos are produced by supernova explosions; the flux from the 1987 event is shown. The figure displays the measured atmospheric-neutrino flux up to energies of 100 TeV by the AMANDA experiment [16]. Atmospheric neutrinos are a key to our story, because they are the dominant background for extraterrestrial searches. The flux of atmospheric neutrinos falls dramatically with increasing energy; events above 100 TeV are rare, leaving a clear field of view for extraterrestrial sources.

The highest energy neutrinos in Figure 1 are the decay products of pions produced by the interactions of cosmic rays with microwave photons [17]. Above a threshold of $\sim 4 \times 10^{19}$ eV, cosmic rays interact with the microwave background introducing an absorption feature in the cosmic-ray flux, the Greisen-Zatsepin-Kuzmin (GZK) cut-off. As a consequence, the mean free path of extragalactic cosmic rays propagating in the microwave background is limited to roughly 75 megaparsecs, and therefore, the secondary neutrinos are the only probe of the still-enigmatic sources at longer distances. What they will reveal is a matter of speculation. The calculation of the neutrino flux associated with the observed flux of extragalactic cosmic rays is straightforward and yields one event per year in a kilometer-scale detector. The flux, labeled GZK in Figure 1, shares the high-energy neutrino sky with neutrinos from gamma-ray bursts and active galactic nuclei [4–6].

2. The Cosmic-Ray Puzzle

Despite their discovery potential touching a wide range of scientific issues, the construction of ground-based gamma-ray telescopes and kilometer-scale neutrino detectors has been largely motivated by the possibility of opening a new window on the Universe in the TeV energy region and above. In this paper, we will revisit the prospects for detecting gamma rays and neutrinos associated with cosmic rays, thus revealing their sources at a time when we are commemorating the 100th anniversary of their discovery by Victor Hess in 1912. Unlike charges, cosmic rays, gamma rays, and neutrinos point back at their sources.

Cosmic accelerators produce particles with energies in excess of 10^8 TeV; we still do not know where or how [18–20]. The flux of cosmic rays observed at the Earth is shown

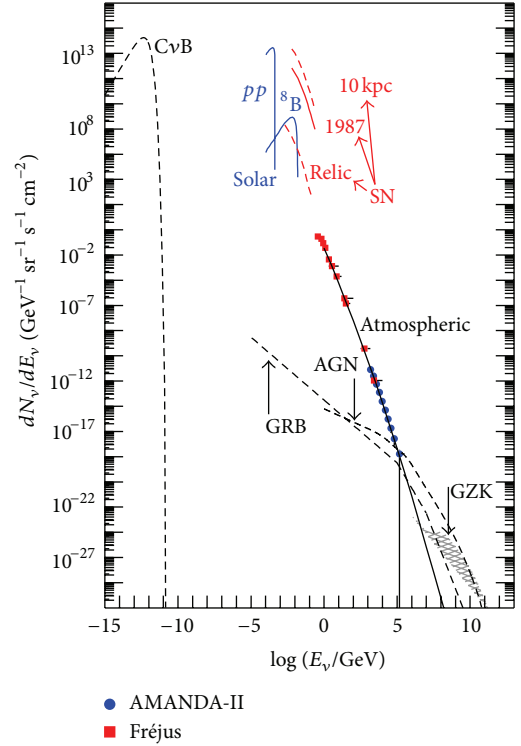


FIGURE 1: The cosmic-neutrino spectrum. Sources are the Big Bang (CvB), the Sun, supernovae (SN), atmospheric neutrinos, active galactic nuclei (AGN) galaxies, and GZK neutrinos. The data points are from detectors at the Fréjus underground laboratory [24] (red) and from AMANDA [16] (blue).

in Figure 2. The energy spectrum follows a sequence of three power laws. The first two are separated by a feature dubbed the “knee” at an energy (we will use energy units TeV, PeV, and EeV, increasing by factors of 1000 from GeV energy) of approximately 3 PeV. There is evidence that cosmic rays up to this energy are Galactic in origin. Any association with our Galaxy disappears in the vicinity of a second feature in the spectrum referred to as the “ankle”; see Figure 2. Above the ankle, the gyroradius of a proton in the Galactic magnetic field exceeds the size of the Galaxy, and we are witnessing the onset of an extragalactic component in the spectrum that extends to energies beyond 100 EeV. Direct support for this assumption now comes from three experiments [21–23] that have observed the telltale structure in the cosmic-ray spectrum resulting from the absorption of the particle flux by the microwave background, the so-called Greisen-Zatsepin-Kuzmin (GZK) cut-off. Neutrinos are produced in GZK interactions; it was already recognized in the 1970s that their observation requires kilometer-scale neutrino detectors. The origin of the cosmic-ray flux in the intermediate region covering PeV-to-EeV energies remains a mystery, although it is routinely assumed that it results from some high-energy extension of the reach of Galactic accelerators.

Acceleration of protons (or nuclei) to TeV energy and above requires massive bulk flows of relativistic charged

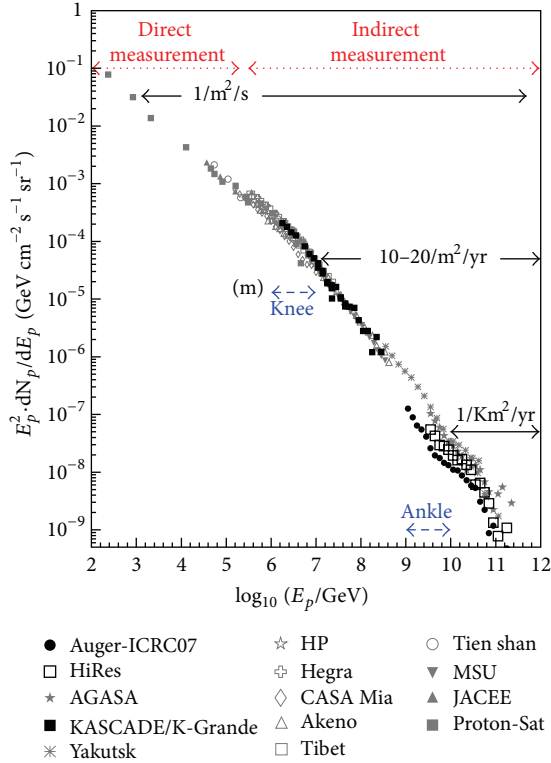


FIGURE 2: At the energies of interest here, the cosmic-ray spectrum follows a sequence of 3 power laws. The first 2 are separated by the “knee,” the 2nd and 3rd by the “ankle.” Cosmic rays beyond the ankle are a new population of particles produced in extragalactic sources.

particles. These are likely to originate from exceptional gravitational forces in the vicinity of black holes or neutron stars. The gravity of the collapsed objects powers large currents of charged particles that are the origin of high magnetic fields. These create the opportunity for particle acceleration by shocks. It is a fact that electrons are accelerated to high energy near black holes; astronomers detect them indirectly by their synchrotron radiation. Some must accelerate protons, because we observe them as cosmic rays.

The detailed blueprint for a cosmic-ray accelerator must meet two challenges: the highest energy particles in the beam must reach $>10^3$ TeV (10^8 TeV) for Galactic (extragalactic) sources and meet the total energy (luminosity) requirement to accommodate the observed cosmic-ray flux. Both represent severe constraints that have limited the imagination of theorists.

Supernova remnants were proposed as possible sources of Galactic cosmic rays as early as 1934 by Baade and Zwicky [25]; their proposal is still a matter of debate after more than 70 years [26]. Galactic cosmic rays reach energies of at least several PeV, the “knee” in the spectrum. Their interactions with Galactic hydrogen in the vicinity of the accelerator should generate gamma rays from the decay of secondary pions that reach energies of hundreds of TeV. Such sources should be identifiable by a relatively flat energy spectrum that extends to hundreds of TeV without attenuation, because

the cosmic rays themselves reach at least several PeV near the knee; they have been dubbed PeVatrons. The search to pinpoint them has so far been unsuccessful.

Although there is no incontrovertible evidence that supernovae accelerate cosmic rays, the idea is generally accepted because of energetics: three supernovae per century converting a reasonable fraction of a solar mass into particle acceleration can accommodate the steady flux of cosmic rays in the Galaxy. Originally, energetics also drove speculations on the origin of extragalactic cosmic rays.

By integrating the cosmic-ray spectrum in Figure 2 above the ankle, we find that the energy density of the Universe in extragalactic cosmic rays is $\sim 3 \times 10^{-19}$ erg cm $^{-3}$ [27, 28]. The power required for a population of sources to generate this energy density over the Hubble time of 10^{10} years is $\sim 3 \times 10^{37}$ erg s $^{-1}$ per (Mpc) 3 . (In the astroparticle community, this flux is also known as 5×10^{44} TeV Mpc $^{-3}$ yr $^{-1}$.) A gamma-ray burst (GRB) fireball converts a fraction of a solar mass into the acceleration of electrons, seen as synchrotron photons. The energy in extragalactic cosmic rays can be accommodated with the reasonable assumption that shocks in the expanding GRB fireball convert roughly equal energy into the acceleration of electrons and cosmic rays [29–31]. It so happens that $\sim 2 \times 10^{52}$ erg per GRB will yield the observed energy density in cosmic rays after 10^{10} years, given that the rate is of order 300 per Gpc 3 per year. Hundreds of bursts per year over Hubble time produce the observed cosmic-ray density, just like the three supernovae per century accommodate the steady flux in the Galaxy.

Problem solved? Not really: it turns out that the same result can be achieved assuming that active galactic nuclei (AGN) convert, on average, $\sim 2 \times 10^{44}$ erg s $^{-1}$ each into particle acceleration. As is the case for GRB, this is an amount that matches their output in electromagnetic radiation. Whether GRB or AGN, the observation that these sources radiate similar energies in photons and cosmic rays is unlikely to be an accident. We will discuss the connection next; it will lead to a prediction of the neutrino flux.

3. Neutrinos (and Photons) Associated with Cosmic Rays

How many gamma rays and neutrinos are produced in association with the cosmic-ray beam? Generically, a cosmic-ray source should also be a beam dump. Cosmic rays accelerated in regions of high magnetic fields near black holes inevitably interact with radiation surrounding them, for example, UV photons in active galaxies or MeV photons in GRB fireballs. In these interactions, neutral and charged pion secondaries are produced by the processes

$$p + \gamma \longrightarrow \Delta^+ \longrightarrow \pi^0 + p, \quad p + \gamma \longrightarrow \Delta^+ \longrightarrow \pi^+ + n. \quad (1)$$

While secondary protons may remain trapped in the high magnetic fields, neutrons and the decay products of neutral and charged pions escape. The energy escaping the source is, therefore, distributed among cosmic rays, gamma rays, and

neutrinos produced by the decay of neutrons, neutral pions, and charged pions, respectively.

In the case of Galactic supernova shocks, discussed further on, cosmic rays mostly interact with the hydrogen in the Galactic disk, producing equal numbers of pions of all three charges in hadronic collisions $p + p \rightarrow n[\pi^0 + \pi^+ + \pi^-] + X$; n is the pion multiplicity. These secondary fluxes should be boosted by the interaction of the cosmic rays with high-density molecular clouds that are ubiquitous in the star-forming regions where supernovae are more likely to explode. A similar mechanism may be relevant to extragalactic accelerators; here we will concentrate on the $p\gamma$ mechanism, relevant, for instance, to GRB.

In a generic cosmic beam dump, accelerated cosmic rays, assumed to be protons for illustration, interact with a photon target. These may be photons radiated by the accretion disk in AGN and synchrotron photons that coexist with protons in the exploding fireball producing a GRB. Their interactions produce charged and neutral pions according to (1), with probabilities $2/3$ and $1/3$, respectively. Subsequently, the pions decay into gamma rays and neutrinos that carry, on average, $1/2$ and $1/4$ of the energy of the parent pion. We here assume that the four leptons in the decay $\pi^+ \rightarrow \nu_\mu + \mu^+ \rightarrow \nu_\mu + (e^+ + \bar{\nu}_\mu)$ equally share the charged pion's energy. The energy of the pionic leptons relative to the proton is

$$x_\nu = \frac{E_\nu}{E_p} = \frac{1}{4} \langle x_{p \rightarrow \pi} \rangle \simeq \frac{1}{20}, \quad (2)$$

$$x_\gamma = \frac{E_\gamma}{E_p} = \frac{1}{2} \langle x_{p \rightarrow \pi} \rangle \simeq \frac{1}{10}. \quad (3)$$

Here,

$$\langle x_{p \rightarrow \pi} \rangle = \left\langle \frac{E_\pi}{E_p} \right\rangle \simeq 0.2 \quad (4)$$

is the average energy transferred from the proton to the pion. The secondary neutrino and photon fluxes are

$$\frac{dN_\nu}{dE} = 1 \frac{1}{3} \frac{1}{x_\nu} \frac{dN_p}{dE_p} \left(\frac{E}{x_\nu} \right), \quad (5)$$

$$\frac{dN_\gamma}{dE} = 2 \frac{2}{3} \frac{1}{x_\gamma} \frac{dN_p}{dE_p} \left(\frac{E}{x_\gamma} \right) = \frac{1}{8} \frac{dN_\nu}{dE}. \quad (6)$$

Here, $N_\nu (= N_{\nu_\mu} = N_{\nu_e} = N_{\nu_\tau})$ represents the sum of the neutrino and antineutrino fluxes which are not distinguished by the experiments. Oscillations over cosmic baselines yield approximately equal fluxes for the 3 flavors.

It is important to realize that the high-energy protons may stay magnetically confined to the accelerator. This is difficult to avoid in the case of a GRB where they adiabatically lose their energy and trapped inside the fireball that expands under radiation pressure until it becomes transparent and produces the display observed by astronomers. Secondary neutrons (see (1)) do escape with high energies and decay

into protons that are the source of the observed extragalactic cosmic-ray flux:

$$\frac{dN_n}{dE} = 1 \frac{1}{3} \frac{1}{x_n} \frac{dN_p}{dE_p} \left(\frac{E}{x_n} \right), \quad (7)$$

with $x_n = 1/2$, the relative energy of the secondary neutron and the initial proton. For an accelerator blueprint where the accelerated protons escape with high energy, the energy in neutrinos is instead given by (5):

$$E^2 \frac{dN_\nu}{dE} = \frac{1}{3} x_\nu E_p^2 \frac{dN_p}{dE_p} (E_p) \quad (8)$$

resulting in a reduced neutrino flux compared to the neutron case. Identifying the observed cosmic-ray flux with the secondary neutron flux enhances the associated neutrino flux. For an accelerator with a generic E^{-2} shock spectrum where $E_p^2 dN_p/dE_p$, the energy of the particles, is constant, the neutron scenario leads to an increased neutrino flux by a factor $3/x_n \simeq 6$.

3.1. Discussion. The straightforward connection between the cosmic-ray, photon, and neutrino fluxes is subject to modification, both for particle-physics, and astrophysics reasons. From the particle-physic point of view, we assume that the initial proton interacts once and only once. If it interacts n_{int} times, a number that depends on the photon target density, (8), is generalized to

$$E_\nu^2 \frac{dN_\nu}{dE_\nu} = [1 - (1 - e^{-n_{\text{int}}})] \frac{1}{3} x_\nu E_p^2 \frac{dN_p}{dE_p} (E_p) f_{\text{GZK}} \quad (9)$$

$$\simeq n_{\text{int}} x_\nu E_p^2 \frac{dN_p}{dE_p} (E_p),$$

for n_{int} that is not too large. The additional factor $f_{\text{GZK}} \simeq 3$ takes into account the fact that neutrinos, unlike protons, are not absorbed by the microwave background, and therefore, reach us from accelerators beyond a GZK proton absorption length of about 50 Mpc. The factor does vary with the specific redshift evolution of the sources considered. Waxman and Bahcall [29], Vietri [30], and Böttcher and Dermer [31] argued that for sources that are transparent to TeV gamma rays, the photon density is such that $n_{\text{int}} < 1$ for protons, the heralded bound; indeed, the cross sections are such that the mean free path of photons by $\gamma\gamma$ interactions at TeV energy is the same as for protons by $p\gamma$ interactions at EeV. (For some reason, the factor $1/3$ in (9) has been replaced by $1/2$ in the original bound.) As was previously discussed, where secondary neutrons are the origin of the observed cosmic rays, the bound is increased. Sources with $n_{\text{int}} > 1$ are referred to as obscured or hidden sources hidden in light, that is, Because IceCube has reached the upper limits of energy in cosmic neutrinos that are below either version of the bound, hidden sources do not exist, at least not the $p\gamma$ version.

One can include photoproduction final states beyond the Δ -resonance approximation that has been presented here [32].

There are also astrophysical issues obscuring the gamma-neutrino connection of (9), which only applies to the gamma-ray flux of pionic origin. Nonthermal sources produce gamma rays by synchrotron radiation, and their TeV fluxes can be routinely accommodated by scattering the photons on the electron beam to higher energy. Separating them from pionic photons has been somewhat elusive, and any application of (9) requires care.

The rationale for kilometer-scale neutrino detectors is that their sensitivity is sufficient to reveal generic cosmic-ray sources with an energy density in neutrinos comparable to their energy density in cosmic rays [27, 28] and pionic TeV gamma rays [33, 34].

4. Sources of Galactic Cosmic Rays

The energy density of the cosmic rays in our Galaxy is $\rho_E \sim 10^{-12} \text{ erg cm}^{-3}$. Galactic cosmic rays are not forever; they diffuse within the microgauss fields and remain trapped for an average containment time of 3×10^6 years. The power needed to maintain a steady energy density requires accelerators delivering 10^{41} erg/s . This happens to be 10% of the power produced by supernovae releasing 10^{51} erg every 30 years (10^{51} erg correspond to 1% of the binding energy of a neutron star after 99% is initially lost to neutrinos). This coincidence is the basis for the idea that shocks produced by supernovae exploding into the interstellar medium are the accelerators of the Galactic cosmic rays.

Despite the rapid development of instruments with improved sensitivity, it has been impossible to conclusively pinpoint supernova remnants as the sources of cosmic rays by identifying accompanying gamma rays of pion origin. A generic supernova remnant releasing an energy of $W \sim 10^{50} \text{ erg}$ into the acceleration of cosmic rays will inevitably generate TeV gamma rays by interacting with the hydrogen in the Galactic disk. The emissivity in pionic gamma rays Q_γ is simply proportional to the density of cosmic rays n_{cr} and to the target density n of hydrogen atoms. Here, $n_{\text{cr}} \approx 4 \times 10^{-14} \text{ cm}^{-3}$ is obtained by integrating the proton spectrum for energies in excess of 1 TeV. For an E^{-2} spectrum,

$$Q_\gamma \approx c \left\langle \frac{E_\pi}{E_p} \right\rangle \lambda_{pp}^{-1} n_{\text{cr}} (> 1 \text{ TeV}) \approx 2c x_\gamma \sigma_{pp} n n_{\text{cr}}, \quad (10)$$

or

$$Q_\gamma (> 1 \text{ TeV}) \approx 10^{-29} \frac{\text{photons}}{\text{cm}^3 \text{ s}} \left(\frac{n}{1 \text{ cm}^{-3}} \right). \quad (11)$$

The proportionality factor in (10) is determined by particle physics; x_γ is the average energy of secondary photons relative to the cosmic-ray protons, and $\lambda_{pp} = (n\sigma_{pp})^{-1}$ is the proton interaction length ($\sigma_{pp} \approx 40 \text{ mb}$) in a density n of hydrogen atoms. The corresponding luminosity is

$$L_\gamma (> 1 \text{ TeV}) \approx Q_\gamma \frac{W}{\rho_E}, \quad (12)$$

where W/ρ_E is the volume occupied by the supernova remnant. We here made the approximation that the volume of the

young remnant is approximately given by W/ρ_E or that the density of particles in the remnant is not very different from the ambient energy density $\rho_E \sim 10^{-12} \text{ erg cm}^{-3}$ of Galactic cosmic rays [4–6].

We thus predict [35, 36] a rate of TeV photons from a supernova at a nominal distance d of order 1 kpc of

$$\begin{aligned} \int_{E>1 \text{ TeV}} \frac{dN_\gamma}{dE_\gamma} dE_\gamma &= \frac{L_\gamma (> 1 \text{ TeV})}{4\pi d^2} \\ &\approx 10^{-12} - 10^{-11} \left(\frac{\text{photons}}{\text{cm}^2 \text{ s}} \right) \\ &\times \left(\frac{W}{10^{50} \text{ erg}} \right) \left(\frac{n}{1 \text{ cm}^{-3}} \right) \left(\frac{d}{1 \text{ kpc}} \right)^{-2}. \end{aligned} \quad (13)$$

As discussed in the introduction, the position of the knee in the cosmic-ray spectrum indicates that some sources accelerate cosmic rays to energies of several PeV. These PeVatrons, therefore, produce pionic gamma rays whose spectrum can extend to several hundred TeV without cutting off. For such sources, the γ -ray flux in the TeV energy range can be parametrized in terms of a spectral slope α_γ , an energy $E_{\text{cut},\gamma}$ where the accelerator cuts off and a normalization k_γ

$$\frac{dN_\gamma(E_\gamma)}{dE_\gamma} = k_\gamma \left(\frac{E_\gamma}{\text{TeV}} \right)^{-\alpha_\gamma} \exp \left(-\sqrt{\frac{E_\gamma}{E_{\text{cut},\gamma}}} \right). \quad (14)$$

The estimate in (13) indicates that fluxes as large as $dN_\gamma/dE_\gamma \sim 10^{-12} - 10^{-14} (\text{TeV}^{-1} \text{ cm}^{-2} \text{ s}^{-1})$ can be expected at energies of $\mathcal{O}(10 \text{ TeV})$.

We, therefore, concentrate on the search for PeVatrons, supernova remnants with the required energetics to produce cosmic rays, at least up to the “knee” in the spectrum. They may have been revealed by the highest energy all-sky survey in $\sim 10 \text{ TeV}$ gamma rays from the Milagro detector [37]. A subset of sources, located within nearby star-forming regions in Cygnus and in the vicinity of Galactic latitude $l = 40$ degrees, are identified; some cannot be readily associated with known supernova remnants or with nonthermal sources observed at other wavelengths. Subsequently, directional air Cherenkov telescopes were pointed at three of the sources, revealing them as PeVatron candidates with an approximate E^{-2} energy spectrum that extends to tens of TeV without evidence for a cut-off [38, 39], in contrast with the best studied supernova remnants RX J1713-3946 and RX J0852.0-4622 (Vela Junior).

Some Milagro sources may actually be molecular clouds illuminated by the cosmic-ray beam accelerated in young remnants located within $\sim 100 \text{ pc}$. One expects indeed that multi-PeV cosmic rays are accelerated only over a short time period when the shock velocity is high, that is, when the remnant transitions from free expansion to the beginning of the Sedov phase. The high-energy particles can produce photons and neutrinos over much longer periods when they diffuse through the interstellar medium to interact with nearby

molecular clouds [40]. An association of molecular clouds and supernova remnants is expected, of course, in star-forming regions. In this case, any confusion with synchrotron photons is unlikely.

Despite the rapid development of both ground-based and satellite-borne instruments with improved sensitivity, it has been impossible to conclusively pinpoint supernova remnants as the sources of cosmic-ray acceleration by identifying accompanying gamma rays of pion origin. In fact, recent data from Fermi LAT have challenged the hadronic interpretation of the GeV-TeV radiation from one of the best studied candidates, RX J1713-3946 [41]. In contrast, detecting the accompanying neutrinos would provide incontrovertible evidence for cosmic-ray acceleration. Particle physics dictates the relation between pionic gamma rays and neutrinos and basically predicts the production of a $\nu_\mu + \bar{\nu}_\mu$ pair for every two gamma rays seen by Milagro. This calculation can be performed using the formalism discussed in the previous section with approximately the same outcome. Confirmation that some of the Milagro sources produced pionic gamma rays produced by a cosmic-ray beam is predicted to emerge after operating the complete IceCube detector for several years; see Figure 3.

The quantitative statistics can be summarized as follows. For average values of the parameters describing the flux, we find that the completed IceCube detector could confirm sources in the Milagro sky map as sites of cosmic-ray acceleration at the 3σ level in less than one year and at the 5σ level in three years [35]. We here assume that the source extends to 300 TeV or 10% of the energy of the cosmic rays near the knee in the spectrum. These results agree with previous estimates [42, 43]. There are intrinsic ambiguities in this estimate of an astrophysical nature that may reduce or extend the time required for a 5σ observation [35]. Especially, the poorly known extended nature of some of the Milagro sources represents a challenge for IceCube observations that are optimized for point sources. In the absence of observation of TeV-energy supernova neutrinos by IceCube within a period of 10 years, the concept will be challenged.

5. Sources of the Extragalactic Cosmic Rays

Unlike the case for Galactic cosmic rays, there is no straightforward γ -ray path to the neutrino flux expected from extragalactic cosmic-ray accelerators. Neutrino fluxes from AGN are difficult to estimate. For GRB, the situation is qualitatively better, because neutrinos of PeV energy should be produced when protons and photons coexist in the GRB fireball [29]. As previously discussed, the model is credible because the observed cosmic-ray flux can be accommodated with the assumption that roughly equal energy is shared by electrons, observed as synchrotron photons and protons.

5.1. GRB. If GRB fireballs are the sources of extragalactic cosmic rays, the neutrino flux is directly related to the cosmic-ray flux. The relation follows from the fact that, for each

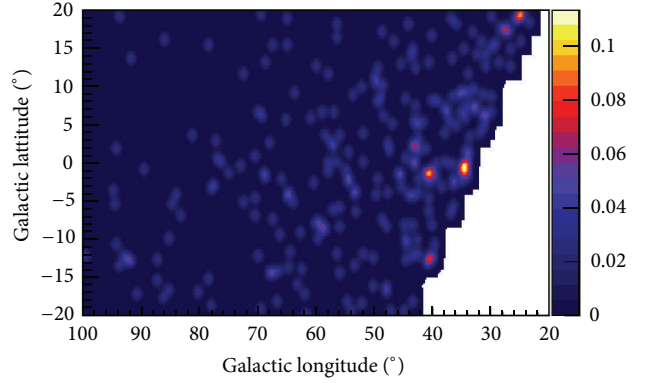


FIGURE 3: Simulated sky map of IceCube in Galactic coordinates after 5 years of operation of the completed detector. Two Milagro sources are visible with 4 events for MGRO J1852 + 01 and 3 events for MGRO J1908 + 06 with energy in excess of 40 TeV. These, as well as the background events, have been randomly distributed according to the resolution of the detector and the size of the sources.

secondary neutron decaying into a cosmic-ray proton, there are 3 neutrinos produced from the associated π^+ :

$$E \frac{dN_\nu}{dE} = 3E_n \frac{dN_n}{dE_n}(E_n), \quad (15)$$

and, after oscillations, per neutrino flavor

$$E^2 \frac{dN_\nu}{dE} \simeq \left(\frac{x_\nu}{x_n} \right) E_n^2 \frac{dN_n}{dE_n}(E_n) f_{\text{GZK}}, \quad (16)$$

where the factor f_{GZK} is introduced for reasons explained in the context of (9).

An alternative approach is followed in routine IceCube GRB searches [44]: the proton content of the fireball is derived from the observed electromagnetic emission (the Band spectrum). The basic assumption is that a comparable amount of energy is dissipated in fireball protons and electrons, where the latter are observed as synchrotron radiation:

$$E^2 \frac{dN_\nu}{dE} = \left(\frac{\epsilon_p}{\epsilon_e} \right) \frac{1}{2} x_\nu \left[E_\gamma^2 \frac{dN_\gamma}{dE_\gamma}(E_\gamma) \right]_{\text{syn}}, \quad (17)$$

where ϵ_p , ϵ_e are the energy fractions in the fireball in protons and electrons [44].

The critical quantity normalizing the GRB neutrino flux is n_{int} ; its calculation is relatively straightforward. The phenomenology that successfully accommodates the astronomical observations is that of the creation of a hot fireball of electrons, photons, and protons that is initially opaque to radiation. The hot plasma, therefore, expands by radiation pressure, and particles are accelerated to a Lorentz factor Γ that grows until the plasma becomes optically thin and produces the GRB display. From this point on, the fireball coasts with a Lorentz factor that is constant and depends on its baryonic load. The baryonic component carries the bulk of the fireball's kinetic energy. The energetics and rapid

time structure of the burst can be successfully associated with successive shocks (shells), of width ΔR , that develop in the expanding fireball. The rapid temporal variation of the gamma-ray burst, t_v , is of the order of milliseconds and can be interpreted as the collision of internal shocks with a varying baryonic load leading to differences in the bulk Lorentz factor. Electrons, accelerated by the first-order Fermi acceleration, radiate synchrotron gamma rays in the strong internal magnetic field and thus produce the spikes observed in the burst spectra.

The number of interactions is determined by the optical depth of the fireball shells to py interactions

$$n'_{\text{int}} = \frac{\Delta R'}{\lambda_{py}} = (\Gamma c t_v) (n'_\gamma \sigma_{py}). \quad (18)$$

The primes refer to the fireball rest frame; unprimed quantities are in the observer frame. The density of fireball photons depends on the total energy in the burst $E_{\text{GRB}} \approx 2 \times 10^{52}$ erg, the characteristic photon energy of $E_\gamma \approx 1$ MeV, and the volume V' of the shell:

$$n'_\gamma = \frac{E_{\text{GRB}}/E_\gamma}{V'}, \quad (19)$$

with

$$V' = 4\pi R'^2 \Delta R' = 4\pi (\Gamma^2 c t_v)^2 (\Gamma c t_v). \quad (20)$$

The only subtlety here is the Γ^2 dependence of the shell radius R' ; for a simple derivation see Gaisser et al. [4], Learned and Mannheim [5], and Halzen and Hooper [6]. Finally, note that this calculation identifies the cosmic-ray flux with the fireball protons.

The back-of-the-envelope prediction for the GRB flux is given by (9) with $n_{\text{int}} \approx 1$, or

$$E^2 \frac{dN_\nu}{dE} \approx \frac{1}{3} x_\nu E_p^2 \frac{dN_p}{dE_p} (E_n) f_{\text{GZK}} \approx x_\nu E_p^2 \frac{dN_p}{dE_p} (E_n). \quad (21)$$

If one identifies the proton flux with neutrons escaping from the fireball, the calculation should be based on (16). This is almost certainly the correct procedure, as the protons lose their energy adiabatically with the expansion of the fireball. The neutrino flux is increased by a factor of approximately $3/x_n \approx 6$. This more straightforward approach has been pursued by Ahlers et al. [45].

For typical choices of the parameters, $\Gamma \sim 300$ and $t_v \sim 10^{-2}$ s, about 100 events per year are predicted in IceCube, a flux that is already challenged [45] by the limit on a diffuse flux of cosmic neutrinos obtained with one-half of IceCube in one year [46]. Facing this negative conclusion, Ahlers et al. [45] have investigated the dependence of the predicted neutrino flux on the cosmological evolution of the sources, as well as on the parameters describing the fireball, most notably E_{GRB} , Γ , and t_v . Although these are constrained by the electromagnetic observations, and by the requirement that the fireball must accommodate the observed cosmic-ray spectrum, the predictions can be stretched to the point that it

will take 3 years of data with the now-completed instrument to conclusively rule out the GRB origin of the extragalactic cosmic rays; see Figure 4. Alternatively, detection of their neutrino emission may be imminent.

Is the GRB origin of sources of the highest energy cosmic rays challenged? Recall that calculation of the GRB neutrino flux is normalized to the observed total energy in extragalactic cosmic rays of $\sim 3 \times 10^{-19}$ erg cm $^{-3}$, a value that is highly uncertain because it critically depends on the assumption that all cosmic rays above the ankle are extragalactic in origin. Also, the absolute normalization of the measured flux is uncertain. Although fits to the spectrum support this assumption [45], by artificially shifting the transition to higher energies above the knee, one can reduce the energy budget by as much as an order of magnitude. The lower value of 0.5×10^{44} TeV Mpc $^{-3}$ yr $^{-1}$ can be accommodated with a more modest fraction of $\sim 2 \times 10^{51}$ erg (or $\sim 1\%$ of a solar mass) going into particle acceleration in individual bursts. We will revisit this issue in the context of GZK neutrinos.

While this temporarily remedies the direct conflict with the present diffuse limit, IceCube has the alternative possibility to perform a direct search for neutrinos in spatial and time coincidence with GRB observed by the Swift and Fermi satellites; its sensitivity is superior by over one order of magnitude relative to a diffuse search. In this essentially background-free search, 14 events were expected when IceCube operated with 40 and 59 strings during 2 years of construction, even for the lowest value of the cosmic-ray energy budget of 0.5×10^{44} TeV Mpc $^{-3}$ yr $^{-1}$. Two different and independent searches failed to observe this flux at the 90% confidence level [47]. IceCube has the potential to confirm or rule out GRB as the sources of the highest energy cosmic rays within 3 years of operation [45].

5.2. Active Galaxies. If, alternatively, AGN were the sources, we are in a situation where a plethora of models have produced a wide range of predictions for the neutrino fluxes; these range from unobservable to ruled out by IceCube data taken during construction. We, therefore, will follow the more straightforward path of deriving the neutrino flux from the TeV gamma-ray observations, as was done for supernova remnants. This approach is subject to the usual caveat that some, or all, of the photons may not be pionic in origin; in this sense, the estimate provides an upper limit. The proximity of the Fanaroff-Riley I (FRI) active galaxies Cen A and M 87 singles them out as potential accelerators [48, 49]. The Auger data provide suggestive evidence for a possible correlation between the arrival direction of 1–10 events and the direction of Cen A [48].

Interpreting the TeV gamma-ray observations is challenging because the high-energy emission of AGN is extremely variable, and it is difficult to compare multiwavelength data taken at different times. Our best guess is captured in Figure 5 where the TeV flux is shown along with observations of the multiwavelength emission of Cen A compiled by Lipari [50].

The TeV flux shown represents an envelope of observations.

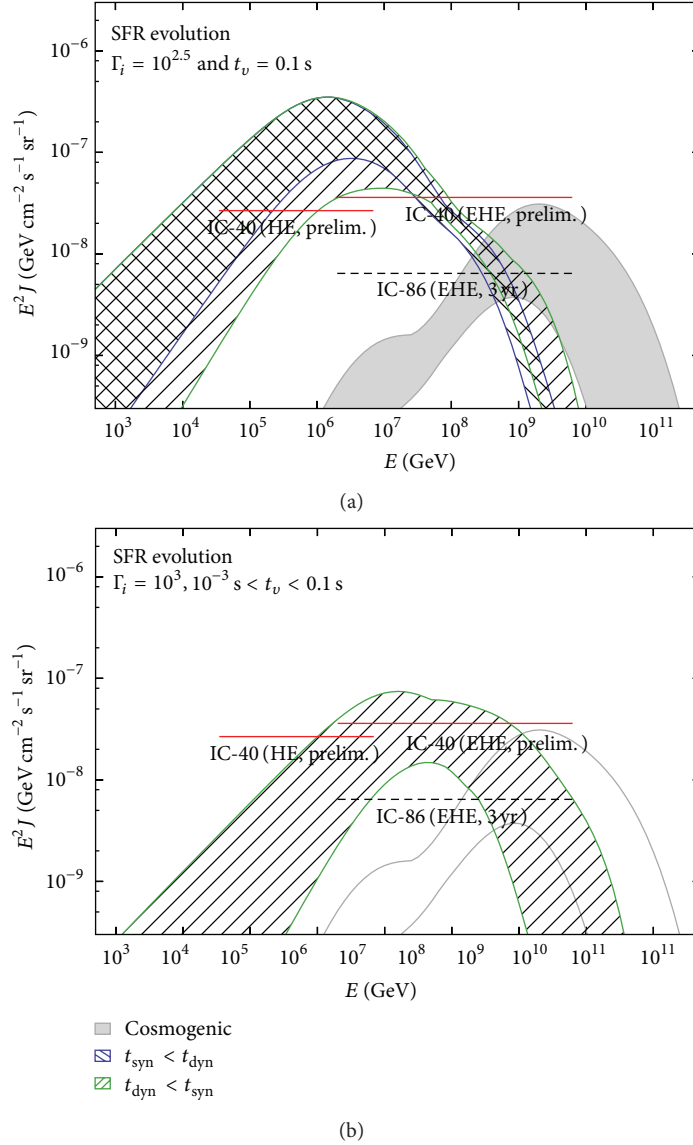


FIGURE 4: GRB neutrino spectra (the prompt spectrum emitted by the sources and neutrino spectrum generated in GZK interactions are shown separately), assuming the luminosity range $0.1 < (\epsilon_B/\epsilon_e)L_{\gamma,52} < 10$ and star-forming redshift evolution of the sources. Here, $\epsilon_{e,B}$ are the fractional energies in the fireball carried by the electrons and the magnetic field; the two are equal in the case of equipartition. $L_{\gamma,52}$ is the photon energy in units of 10^{52} erg. We show the prompt spectra separately for models where the fireball's dynamical time scale t_{dyn} is smaller (larger) than the synchrotron loss time scale t_{syn} (green right-hatched and blue cross-hatched, resp.). Here, the dynamical time scale is just the variability scale $t_{\text{dyn}} = t_v$ and $t'_{\text{dyn}} = t_v \Gamma$. The IceCube limits [46] on the total neutrino flux from the analysis of high-energy and ultra-high-energy muon neutrinos with the 40-string subarray assume 1 : 1 : 1 flavor composition after oscillation. We also show the sensitivity of the full IceCube detector (IC-86) to muon neutrinos after 3 years of observation. The gray solid area shows the range of GZK neutrinos expected at the 99% C.L.

- (1) Archival observations of TeV emission of Cen A collected in the early 1970s with the Narrabri optical intensity interferometer of the University of Sydney [51–53]. The data show variability of the sources over periods of one year.
- (2) Observation by HEGRA [54–59] of M 87. We scaled the flux of M 87 at 16 Mpc to the distance to Cen A. After adjusting for the different thresholds of the HEGRA and Sydney experiments, we obtain

identical source luminosities for M 87 and Cen A of roughly $7 \times 10^{40} \text{ erg s}^{-1}$, assuming an E^{-2} gamma-ray spectrum.

- (3) And, most importantly, the time-averaged gamma-ray flux thus obtained is very close to the gamma-ray flux from Cen A recently observed at the $3\sim 4\sigma$ level by the H.E.S.S. collaboration [60].

Given that we obtain identical intrinsic luminosities for Cen A and M 87, we venture the assumption that they may

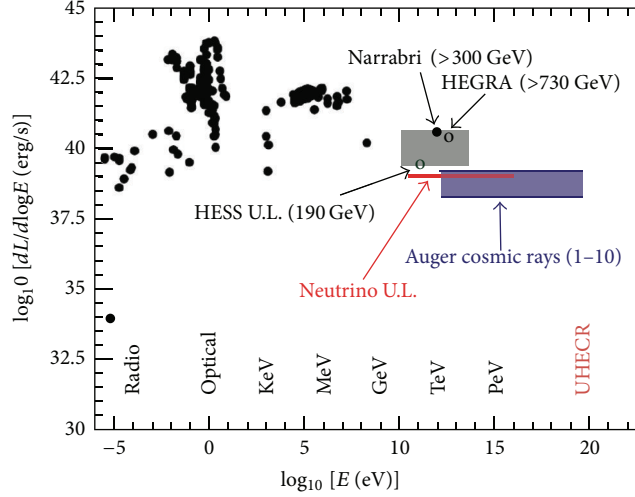


FIGURE 5: Spectral energy distribution of Cen A (black dots). Keeping in mind that the source is variable, we show our estimates for the flux of TeV gamma rays (upper gray shading) and cosmic rays assuming that between 1 and 10 events observed by Auger originated at Cen A (lower blue shading). We note that cosmic-ray and TeV gamma-ray fluxes estimated in this paper are at a level of the electromagnetic component shown from radio waves to GeV photons. Our estimate for the neutrino flux (labeled “neutrino upper limit”; see text) is shown as the red line.

be generic FRI, a fact that can be exploited to construct the diffuse neutrino flux from all FRI. The straightforward conversion of the TeV gamma-ray flux from a generic FRI to a neutrino flux yields

$$\frac{dN_\nu}{dE} \approx 5 \times 10^{-13} \left(\frac{E}{\text{TeV}} \right)^{-2} \text{TeV}^{-1} \text{cm}^{-2} \text{s}^{-1}. \quad (22)$$

The total diffuse flux from all such sources with a density of $n \approx 8 \times 10^4 \text{ Gpc}^{-3}$ within a horizon of $R \sim 3 \text{ Gpc}$ [61] is simply the sum of luminosities of the sources weighted by their distance, or

$$\frac{dN_\nu}{dE_{\text{diff}}} = \sum \frac{L_\nu}{4\pi d^2} = L_\nu n R = 4\pi d^2 n R \frac{dN_\nu}{dE}, \quad (23)$$

where dN_ν/dE is given by the single-source flux. We performed the sum by assuming that the galaxies are uniformly distributed. This evaluates to

$$\frac{dN_\nu}{dE_{\text{diff}}} = 2 \times 10^{-12} \left(\frac{E}{\text{TeV}} \right)^{-2} \text{GeV}^{-1} \text{cm}^{-2} \text{s}^{-1} \text{sr}^{-1}. \quad (24)$$

The neutrino flux from a single source such as Cen A is clearly small: repeating the calculation for power-law spectra between 2.0 and 3.0, we obtain, in a generic neutrino detector of effective muon area 1 km^2 , only 0.8 to 0.02 events per year. The diffuse flux yields a more comfortable event rate of between 0.5 and 19 neutrinos per year. Considering sources out to 3 Gpc, or a redshift of order 0.5 only, is probably conservative. Extending the sources beyond $z \sim 1$, and taking into account their possible evolution, may increase the flux by a factor 3 or so.

6. Neutrinos from GZK Interactions

Whatever the sources of extragalactic cosmic rays may be, a cosmogenic flux of neutrinos originates from the interactions

of cosmic rays with the cosmic microwave background (CMB). Produced within a GZK radius by a source located at a cosmological distance, a GZK neutrino points back to it with subdegree precision. The calculation of the GZK neutrino flux is relatively straightforward, and its magnitude is very much determined by their total energy density in the universe; as before, the crossover from the Galactic to the extragalactic component is the critical parameter. Recent calculations [62] are shown in Figure 6. It is also important to realize that, among the $p\gamma$ final state products produced via the decay of pions, GZK neutrinos are accompanied by a flux of electrons, positrons, and γ -rays that quickly cascades to lower energies in the CMB and intergalactic magnetic fields. An electromagnetic cascade develops with a maximum in the GeV-TeV energy region. Here, the total energy in the electromagnetic cascade is constrained by recent Fermi-LAT measurements of the diffuse extragalactic γ -ray background [63].

The increased performance of IceCube at EeV energy has opened the possibility for IceCube to detect GZK neutrinos. We anticipate 2.3 events in 3 years of running the completed IceCube detector, assuming the best fit in Figure 6 and 4.8 events for the highest flux consistent with the Fermi constraint.

Throughout the discussion, we have assumed that the highest energy cosmic rays are protons. Experiments disagree on the composition of particles around 10^{20} eV . Little is known about the chemical composition just below to beyond the GZK cut-off, where the most significant contribution to cosmogenic neutrinos is expected. In any case, uncertainties in extrapolation of the proton-air interaction cross-section, elasticity, and multiplicity of secondaries from accelerator measurements to the high energies characteristic for air showers are large enough to undermine any definite conclusion on the chemical composition [64]. Therefore, the

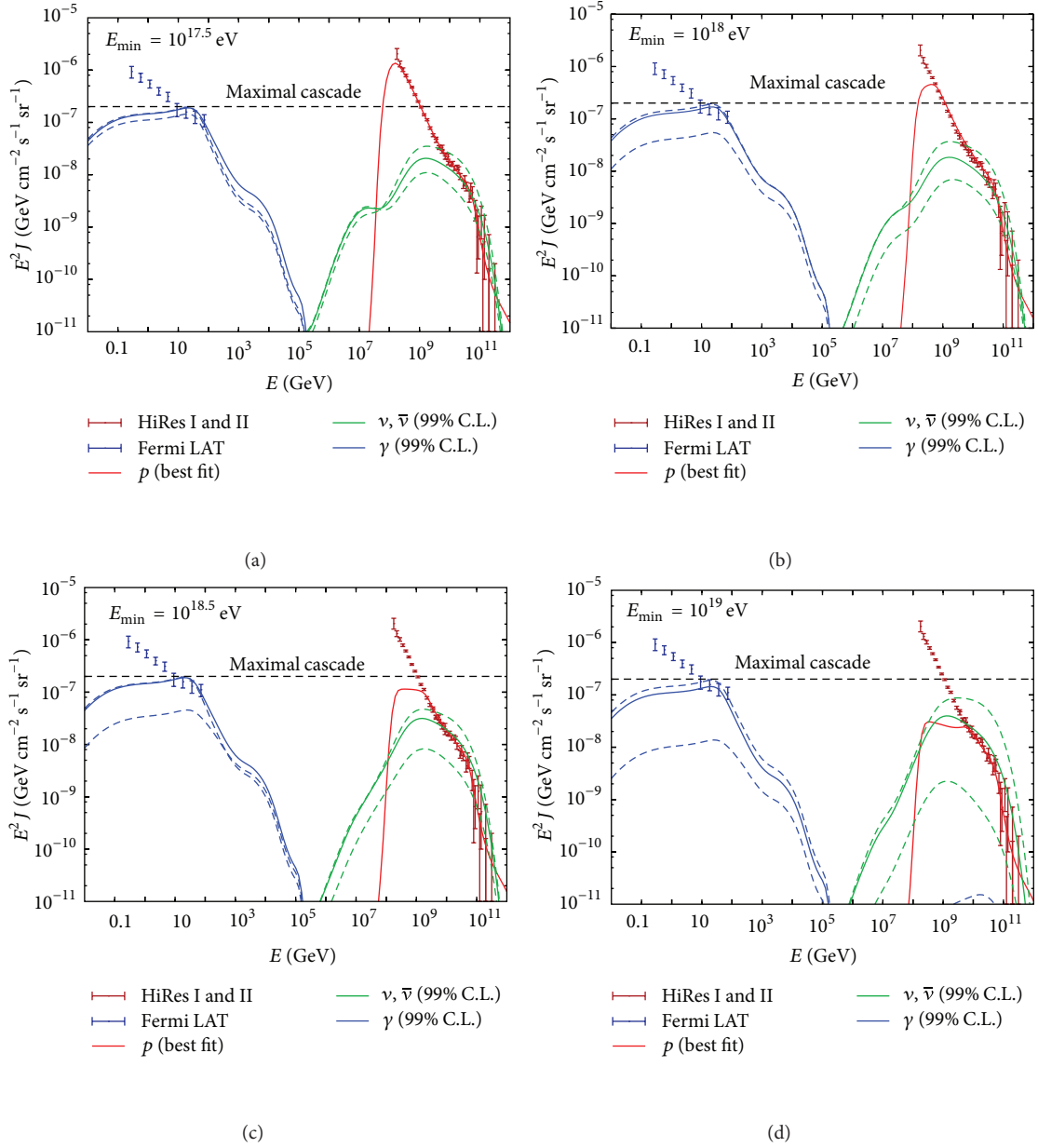


FIGURE 6: Comparison of proton, neutrino, and gamma-ray fluxes produced in interactions on the CMB by cosmic-ray protons fitted to HiRes data. We repeat the calculation for 4 values of the crossover energy marking the transition to the extragalactic cosmic-ray flux. We show the best fit values (solid lines) as well as neutrino and gamma-ray fluxes within the 99% C.L. with minimal and maximal energy density (dashed lines). The γ -ray fluxes are marginally consistent at the 99% C.L. with the highest energy measurements by Fermi-LAT. The contribution around 100 GeV is somewhat uncertain, due to uncertainties in the cosmic infrared background.

conflicting claims by these experiments most likely illustrate that the particle physics is not sufficiently known to derive a definite result. Dedicated experiments at the LHC may remedy this situation by constraining the shower simulations that are a central ingredient in determining the composition.

7. A Comment on the Science Reach of Neutrino “Telescopes”

We have emphasized the potential of IceCube to reveal the sources of the cosmic rays; this goal is clearly of primary

importance as it sets the scale of the detector. IceCube science includes other priorities.

- (1) As for conventional astronomy, neutrino astronomers observe the neutrino sky through the atmosphere. This is a curse and a blessing; the background of neutrinos produced by cosmic rays in interactions with atmospheric nuclei provides a beam essential for calibrating the instrument. It also presents us with an opportunity to do particle physics. Especially unique is the energy range of the background atmospheric neutrino beam covering the interval 1–10⁵ TeV,

energies not within reach of accelerators. Cosmic beams of even higher energy may exist, but the atmospheric beam is guaranteed. IceCube is expected to collect a data set of order one million neutrinos over ten years with a scientific potential that is only limited by our imagination.

- (2) The passage of a large flux of MeV-energy neutrinos produced by a galactic supernova over a period of seconds will be detected as an excess of the background counting rate in all individual optical modules [65]. Although only a counting experiment, IceCube will measure the time profile of a neutrino burst near the center of the Galaxy with a statistics of about one million events, equivalent to the sensitivity of a 2-megaton detector.
- (3) IceCube will search for neutrinos from the annihilation of dark matter particles gravitationally trapped at the center of the Sun and the Earth [66]. In searching for generic weakly interacting massive dark matter particles (WIMPs) with spin-independent interactions with ordinary matter, IceCube is only competitive with direct detection experiments [67] if the WIMP mass is sufficiently large. For spin-dependent interactions, IceCube already has improved the best limits on spin-dependent WIMP cross-sections by two orders of magnitude [68, 69].

Construction of IceCube and other high-energy neutrino telescopes is mostly motivated by their potential to open a new window on the Universe using neutrinos as cosmic messengers; more about this will be in the rest of the talk. The IceCube experiment, nevertheless, appeared on the U.S. Roadmap to Particle Physics [70]. As the lightest of fermions and the most weakly interacting of particles, neutrinos occupy a fragile corner of the standard model, and one can realistically hope that they will reveal the first and the most dramatic signatures of new physics.

Besides its potential to detect dark matter, IceCube's opportunities for particle physics include the following [71].

- (1) The search for signatures of the unification of particle interactions, possibly including gravity at the TeV scale. In this case, neutrinos approaching TeV energies would interact gravitationally with large cross-sections, similar to those of quarks and leptons; this increase yields dramatic signatures in a neutrino telescope including, possibly, the production of black holes [72].
- (2) The search for modifications of neutrino oscillations that result from nonstandard neutrino interactions [73].
- (3) Searching for flavor changes or energy-dependent delays of neutrinos detected from cosmic distances as a signature for quantum decoherence.
- (4) The search for a breakdown of the equivalence principle as a result of nonuniversal interactions with the gravitational field of neutrinos with different flavor.

- (5) Similarly, the search for a breakdown of Lorentz invariance resulting from different limiting velocities of neutrinos of different flavors. With energies of 10^3 TeV and masses of order 10^{-2} eV or less, even the atmospheric neutrinos observed by IceCube reach Lorentz factors of 10^{17} or larger.
- (6) The search for particle emission from cosmic strings or any other topological defects or heavy cosmological remnants created in the early Universe. It has been suggested that they may be the sources of the highest energy cosmic rays.
- (7) The search for magnetic monopoles, nuclearites, Q-balls, and the like.

The DeepCore upgrade of IceCube has significantly extended IceCube's scientific potential as an atmospheric neutrino detector. It will accumulate atmospheric neutrino data covering the first oscillation dip near 20 GeV with unprecedented statistics. Its instrumented volume is of order 10 Mton. With 6 additional strings instrumented with closely spaced (7 meters) high quantum efficiency photomultipliers buried deep inside IceCube, DeepCore uses the surrounding IceCube strings as a veto in order to observe the tracks of contained events; see Figure 7. It has been shown that the event statistics are sufficient to determine the mass hierarchy with at least 90% confidence level assuming the current best-fit values of the oscillation parameters [74]. A positive result does, however, require a sufficient understanding of the systematics of the measurement, and, more realistically, we should ask the question of how many additional strings, deployed within DeepCore, it takes to perform a definite determination. This is a work in progress, not only based on simulations, but also on DeepCore data that have already yielded evidence at the 5σ level for atmospheric oscillations at 10–100 GeV, that is, at higher energy than any previous observation.

The physics behind the hierarchy measurement is the same as for long baseline experiments [75]; the key is to measure the Earth matter effects associated with the angle θ_{13} which governs the transitions between ν_e and $\nu_{\mu,\tau}$. The effective θ_{13} mixing angle in matter in a two-flavor framework is given by

$$\sin^2 2\theta_{13}^m = \frac{\sin^2 2\theta_{13}}{\sin^2 2\theta_{13} + (\cos 2\theta_{13} \pm \sqrt{2}G_F N_e / \Delta_{13})^2}, \quad (25)$$

where the plus (minus) sign refers to (anti) neutrinos. N_e is the electron number density of the Earth, $\sqrt{2}G_F N_e$ (eV) = $7.6 \times 10^{-14} Y_e \rho$ (g/cm³), and Y_e , ρ are the electron fraction and the density of the Earth's interior, respectively. The critical quantity is $\Delta_{13} = (m_1^2 - m_3^2)/2E$; its sign determines the mass hierarchy. The resonance condition is satisfied for neutrino energies of order 15 GeV for the baselines of thousands of kilometers studied in atmospheric neutrino experiments. DeepCore extends the threshold of IceCube to this energy. Both the disappearance of muon neutrinos and the appearance of tau and electron neutrinos can be observed.

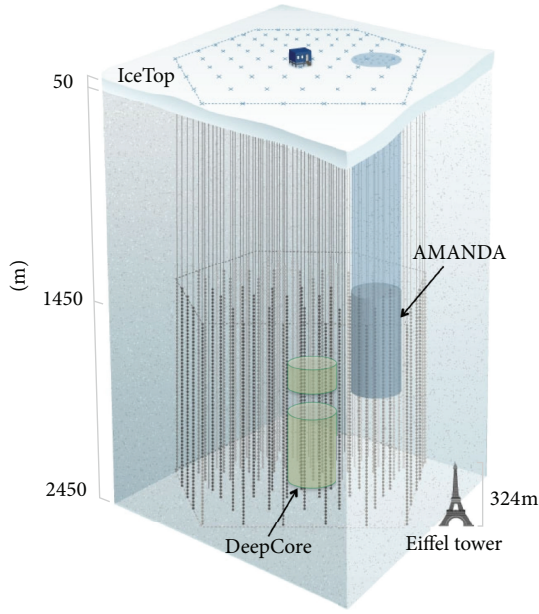


FIGURE 7: The IceCube detector, consisting of IceCube and IceTop and the low-energy sub-detector DeepCore. Also shown is the first-generation AMANDA detector.

In the presence of Earth matter effects, the neutrino (antineutrino) oscillation probability is enhanced if the hierarchy is normal (inverted). Long baseline detectors, unlike IceCube, measure the charge of the secondary muon, thus selecting the sign associated with each event in previous equation. The hierarchy is determined by simply looking in which channel, neutrino or antineutrino, the signal is enhanced by matter effects. With the large value of $\sin^2 2\theta_{13}$, recently observed by several experiments and sufficient statistics, the magnitude of the Δ_{13} term can be measured even without charge discrimination. This is in principle possible with DeepCore [74] or a very modest extension (considering that the cost of an additional string deployed in ice is \$1.2 M, including logistic costs) but cannot be guaranteed until the systematics of the measurement has been fully understood in this newly explored energy range.

8. Neutrino Telescopes: Detection Methods

The detection of neutrinos of all flavors will be important in separating diffuse extraterrestrial neutrinos from atmospheric neutrinos. Generic cosmic accelerators produce neutrinos from the decay of pions with admixture $\nu_e : \nu_\mu : \nu_\tau = 1 : 2 : 0$. Over cosmic baselines, neutrino oscillations transform the ratio to $1 : 1 : 1$, because approximately one-half of the ν_μ convert to ν_τ .

Neutrino telescopes exploit the relatively large neutrino cross-section and the long muon range above TeV energies to achieve a detection efficiency to reach the predicted point source and diffuse fluxes previously discussed. At the same time, detecting ν_e and ν_τ neutrinos cannot be ignored; the case has been made in detail in [13]. The background from atmospheric neutrinos is much lower for ν_e and ν_τ than for

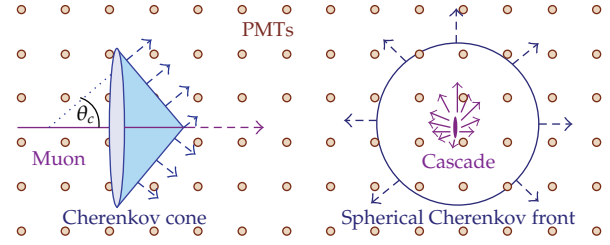


FIGURE 8: Contrasting Cherenkov light patterns produced by muons (left) and by showers initiated by electron and tau neutrinos (right) and by neutral current interactions. The patterns are routinely referred to as tracks and cascades (or showers). Cascades are produced by the radiation of particle showers of dimension of tens of meters, that is, an approximately point source of light with respect to the dimensions of the detector. At PeV energies, τ leptons travel hundreds of meters before decaying, producing a third topology, with two cascades, one when the τ interacts and the second when the τ decays [76]. This is the “double bang” signature.

ν_μ , energy determination is superior because the neutrino event is fully, or at least partially, contained in the detector. For a ν_μ one is limited to sampling the catastrophic energy loss of part of the secondary muon’s track. Finally, they can be detected from both hemispheres, and, as will be discussed further on, ν_τ neutrinos are not absorbed by the Earth, they just cascade to lower energy.

IceCube detects neutrinos by observing the Cherenkov radiation from the charged particles produced by neutrino interactions inside or in the vicinity of the detector. Charge current interactions produce a lepton that carries, on average, 50% of the neutrino energy for $E \leq 10$ GeV to 80% at high energies; the remainder of the energy is released in the form of a hadronic shower. Both the secondary lepton and the hadronic shower produce Cherenkov radiation. In neutral current interactions, the neutrino transfers a fraction of its energy to a nuclear target, producing a hadronic shower. IceCube can differentiate neutrino flavors on the basis of their topology in the detector, as illustrated in Figure 8. There are two basic topologies: tracks from ν_μ and “cascades” from ν_e , ν_τ and the neutral current interactions from all flavors. On the scale of IceCube, cascades are approximately point sources of Cherenkov light. At PeV energies and above, an additional topology is emerges, so-called double-bang events, when a ν_τ interacts producing a cascade and subsequently decays producing a second cascade. At PeV energies, a τ lepton travels hundreds of meters before decaying; this determines the distance between the cascades.

Neutrino telescopes also measure neutrino energy. Muons range out, over kilometers at TeV energy to tens of kilometers at EeV energy, generating showers along their track by bremsstrahlung, pair production, and photonuclear interactions. The charged particles produced are the sources of additional Cherenkov radiation. Because the energy of the muon degrades along its track, also the energy of the secondary showers decreases, and the distance from the track over which the associated Cherenkov light can trigger a PMT is gradually reduced. The geometry of the light pool surrounding the muon track is, therefore, a kilometer-long cone

with a gradually decreasing radius. In its first kilometer, a high-energy muon typically loses energy in a couple of showers of one-tenth of its initial energy. So the initial radius of the cone is the radius of a shower with 10% of the muon energy. At lower energies of hundreds of GeV and less, the muon becomes minimum ionizing.

Because of the stochastic nature of the muon's energy loss, the relationship between observed (via Cherenkov light) energy loss and muon energy varies from muon to muon. The muon energy in the detector can be determined, and beyond that, one does not know how far the muon travelled (and how much energy it lost) before entering the detector; an unfolding process is required to determine the neutrino energy based on the observed muon energies. In contrast, for ν_e and ν_τ , the detector is a total energy calorimeter and the determination of their energy superior.

The different topologies each have advantages and disadvantages. From ν_μ interactions, the long lever arm of muon tracks, up to tens of kilometers at very high energies, allows the muon direction (and the neutrino direction) to be determined accurately with an angular resolution on-line that is better than 0.5 degrees. Superior angular resolution can be reached for selected events. Sensitivity to point sources is, therefore, superior to other flavors. The disadvantages are a large background of atmospheric neutrinos at sub-PeV energies and from cosmic-ray muons at all energies and the indirect determination of the neutrino energy that has to be inferred from sampling the energy loss of the muon when it transits the detector.

Observation of ν_e and ν_τ flavors represents significant observational advantages. They are detected for both Northern and Southern Hemispheres. (This is also true for ν_μ with energy in excess of 1 PeV, where the background from the steeply falling atmospheric spectrum becomes negligible.) At TeV energies and above, the background of atmospheric ν_e is lower by an order of magnitude, and there are almost no atmospheric ν_τ . At higher energies, muons from π decay, the source of atmospheric ν_e , no longer decay, and relatively rare K-decays become the dominant source of background ν_e . Furthermore, because the neutrino events are totally, or at least partially contained inside the instrumented detector volume, the neutrino energy is determined by total absorption calorimetry. One can establish the cosmic origin of a single event by demonstrating that the energy cannot be reached by muons and neutrinos of atmospheric origin. Finally, ν_τ are not absorbed by the Earth [77]: ν_τ interacting in the Earth produce secondary ν_τ of lower energy, either directly in a neutral current interaction or via the decay of a secondary tau lepton produced in a charged current interaction. High-energy ν_τ will thus cascade down to energies of hundred of TeV where the Earth becomes transparent. In other words, they are detected with a reduced energy but are not absorbed.

Although cascades are nearly point-like, they are not isotropic but elliptic with the major axis aligned with the incident neutrino direction. This is reflected in the light pattern detected, especially in the detailed photon signals sampled by the optical sensors. While a fraction of cascade events can be reconstructed with degree accuracy [78], the precision is inferior to the one reached for ν_μ events.

At energies above about 1 PeV in ice, the LPM effect reduces the cross-sections for bremsstrahlung and pair production. At energies above about 10^{17} eV, electromagnetic showers begin to elongate, reaching a length of about 80 meters at 10^{20} eV [79]. At these energies, photonuclear interactions play a role, and even electromagnetic showers will have a hadronic component, including the production of secondary muons.

For an in-depth discussion of neutrino detection, energy measurement and flavor separation, and detailed references, see the IceCube Preliminary Design Document [2, 13].

To a first approximation, neutrinos are detected when they interact inside the instrumented volume. The path length $L(\theta)$ traversed within the detector volume by a neutrino with zenith angle θ is determined by the detector's geometry. Neutrinos are detected if they interact within the detector volume, that is, within the instrumented distance L . That probability is

$$P(E_\nu) = 1 - \exp\left[-\frac{L}{\lambda_\nu(E_\nu)}\right] \approx \frac{L}{\lambda_\nu(E_\nu)}, \quad (26)$$

where $\lambda_\nu(E_\nu) = [\rho_{\text{ice}} N_A \sigma_{\nu N}(E_\nu)]^{-1}$ is the mean free path in ice for a neutrino of energy E_ν . Here $\rho_{\text{ice}} = 0.9 \text{ g cm}^{-3}$ is the density of the ice, $N_A = 6.022 \times 10^{23}$ is Avogadro's number, and $\sigma_{\nu N}(E_\nu)$ is the neutrino-nucleon cross-section. A neutrino flux dN/dE_ν (neutrinos per GeV per cm^2 per second) crossing a detector with energy threshold and cross-sectional area $A(E_\nu)$ facing the incident beam will produce

$$N_{\text{ev}} = T \int_{E_\nu^{\text{th}}} A(E_\nu) P(E_\nu) \frac{dN}{dE_\nu} dE_\nu \quad (27)$$

events after a time T . The "effective" detector area $A(E_\nu)$ is also a function of the zenith angle θ . It is not strictly equal to the geometric cross-section of the instrumented volume facing the incoming neutrino, because even neutrinos interacting outside the instrumented volume may produce enough light inside the detector to be detected. In practice, $A(E_\nu)$ is determined as a function of the incident neutrino direction and zenith angle by a full-detector simulation, including the trigger.

This formalism applies to contained events. For muon neutrinos, any neutrino producing a secondary muon that reaches the detector (and has sufficient energy to trigger it) will be detected. Because the muon travels kilometers at TeV energy and tens of kilometers at PeV energy, neutrinos can be detected outside the instrumented volume; the probability is obtained by substitution in (26):

$$L \longrightarrow \lambda_\mu, \quad (28)$$

therefore,

$$P = \frac{\lambda_\mu}{\lambda_\nu}. \quad (29)$$

Here, λ_μ is the range of the muon determined by its energy losses. The complete expression for the flux of ν_μ -induced

muons at the detector is given by a convolution of the neutrino spectrum $\phi (= dN/dE_\nu)$ with the probability P to produce a muon reaching the detector [4–6]:

$$\begin{aligned} \phi_\mu(E_\mu^{\min}, \theta) \\ = \int_{E_\mu^{\min}} P(E_\nu, E_\mu^{\min}) \exp[-\sigma_{\text{tot}}(E_\nu) N_A X(\theta)] \phi(E_\nu, \theta) dE_\nu. \end{aligned} \quad (30)$$

The additional exponential factor accounts for the absorption of neutrinos along the chord of the Earth of length $X(\theta)$ at zenith angle θ . Absorption becomes important for $\sigma_\nu(E_\nu) \geq 10^{-33} \text{ cm}^2$ or $E_\nu \geq 10^6 \text{ GeV}$. For back-of-the-envelope calculations, the P -function can be approximated by

$$\begin{aligned} P &\approx 1.3 \times 10^{-6} E^{2.2} \quad \text{for } E = 10^{-3} - 1 \text{ TeV} \\ &\approx 1.3 \times 10^{-6} E^{0.8} \quad \text{for } E = 1 - 10^3 \text{ TeV}. \end{aligned} \quad (31)$$

At EeV energy, the increase is reduced to only $E^{0.4}$. Clearly, high-energy neutrinos are more likely to be detected because of the increase with energy of both the cross-section and muon range.

Tau neutrinos can be observed provided that the tau lepton they produce reaches the instrumented volume within its lifetime. In (26), L is replaced by

$$L \longrightarrow \gamma c \tau = \frac{E}{m c \tau}, \quad (32)$$

where m , τ and E are the mass, lifetime, and energy of the tau, respectively. The tau's decay length $\lambda_\tau = \gamma c \tau \approx 50 \text{ m} \times (E_\tau/10^6) \text{ GeV}$ grows linearly with energy and actually exceeds the range of the muon near 1 EeV. At yet higher energies, the tau eventually ranges out by catastrophic interactions, just like the muon, despite the reduction of the cross-sections by a factor $(m_\mu/m_\tau)^2$.

The taus trigger the detector, but the tracks and (or) showers they produce are difficult to be distinguished from those initiated by muon and electron neutrinos. To be clearly recognizable as ν_τ , both the initial neutrino interaction and the subsequent tau decay must be contained within the detector; for a cubic kilometer detector, this happens for neutrinos with energies from a few PeV to a few 10's of PeV. It may also be possible to identify ν_τ that only interact in the detector, or ν_τ that decay in the detector.

9. The First Kilometer-Scale Neutrino Detector: IceCube

The rationale for kilometer-scale neutrino detectors is that their sensitivity is sufficient to reveal generic cosmic-ray sources with an energy density in neutrinos comparable to their energy density in cosmic rays [27, 28] and pionic TeV gamma rays [33, 34]. While TeV gamma-ray astronomy has become a mature technique, the weak link in exploring the multiwavelength opportunities presented previously is the observation of neutrinos that requires detectors of kilometer

scale; this will be demonstrated de facto by the discussion of potential cosmic-ray sources as follows. A series of first-generation experiments [81, 82] have demonstrated that high-energy neutrinos with $\sim 10 \text{ GeV}$ energy and above can be detected by observing Cherenkov radiation from secondary particles produced in neutrino interactions inside large volumes of highly transparent ice or water instrumented with a lattice of photomultiplier tubes. Construction of the first second-generation detector, IceCube, at the geographic South Pole was completed in December 2010 [83]; see Figure 7.

IceCube consists of 80 strings each instrumented with 60 10-inch photomultipliers spaced by 17 m over a total length of 1 kilometer. The deepest module is located at a depth of 2.450 km so that the instrument is shielded from the large background of cosmic rays at the surface by approximately 1.5 km of ice. Strings are arranged at apexes of equilateral triangles that are 125 m on a side. The instrumented detector volume is a cubic kilometer of dark, highly transparent, and sterile Antarctic ice. Radioactive background is dominated by the instrumentation deployed into this natural ice.

Each optical sensor consists of a glass sphere containing the photomultiplier and the electronics board that digitizes the signals locally using an on-board computer. The digitized signals are given a global time stamp with residuals accurate to less than 3 ns and are subsequently transmitted to the surface. Processors at the surface continuously collect these time-stamped signals from the optical modules; each functions independently. The digital messages are sent to a string processor and a global event trigger. They are subsequently sorted into the Cherenkov patterns emitted by secondary muon tracks, or electron and tau showers, that reveal the direction of the parent neutrino [84].

Based on data taken during construction with 40 of the 59 strings, the anticipated effective area of the completed IceCube detector is increased by a factor 2 to 3 over what had been expected [14]. The neutrino collecting area is expected to increase with improved calibration and development of optimized software tools for the 86-string detector, which has been operating stably in its final configuration since May 2011. Already reaching an angular resolution of better than 0.5 degree for high energies, reconstruction is also superior to what was anticipated.

A similar detector, that may eventually be more sensitive than IceCube, is planned for deployment in deep transparent Mediterranean water [85].

10. KM3NeT

Accelerators of cosmic rays produce neutrino fluxes limited in energy to roughly 5% of the maximal energy of the protons or nuclei (see (2)). For Galactic neutrino sources, even the as yet unidentified PeVatrons, we thus expect neutrino spectra with a cut-off (cf. (14)) in the range between a few and about 100 TeV. Detection of these neutrinos thus requires optimized sensitivities in the TeV range. In particular, the atmospheric muon background limits the field of view of neutrino telescopes to the downward hemisphere at these energies.

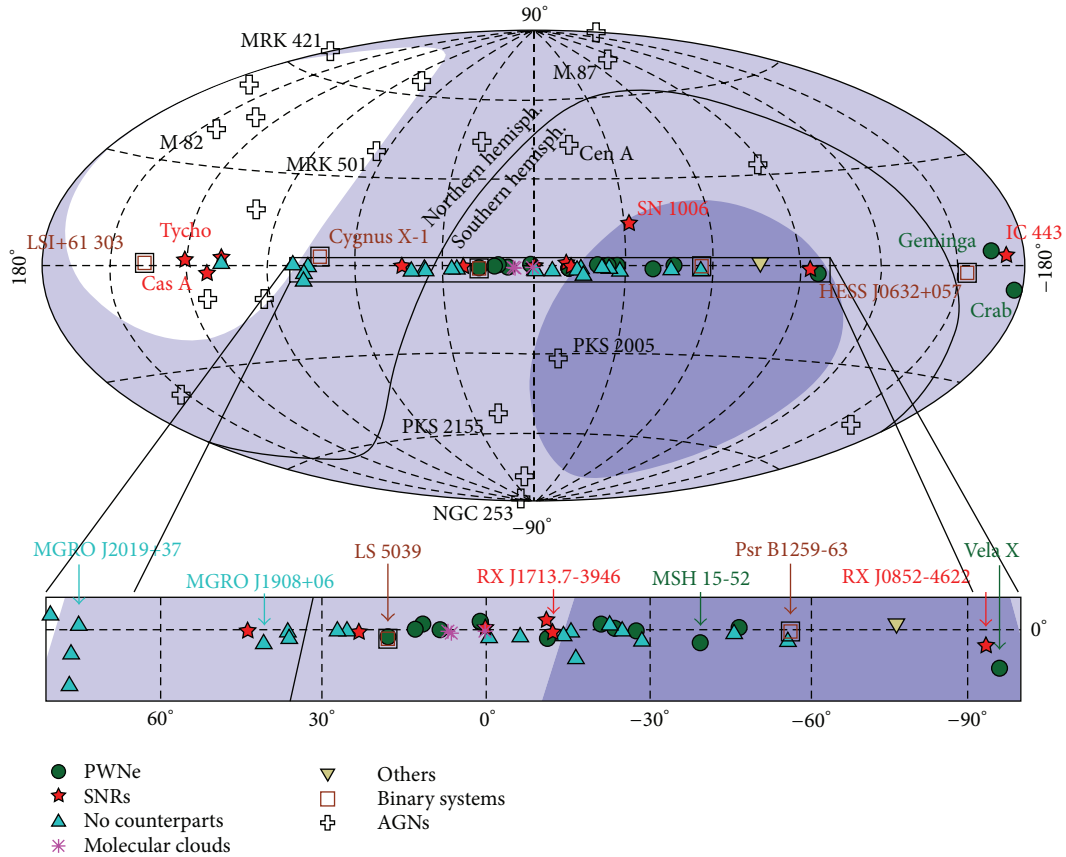


FIGURE 9: Field of view of IceCube (i.e., the Northern hemisphere) and of a Mediterranean-based neutrino telescope in Galactic coordinates. 2π downward sensitivity is assumed. Shades of blue which indicate the fraction of time sources are visible for the Northern telescope (light blue: $>25\%$ of the time; dark blue: $>75\%$ of the time). Also indicated are sources of high-energy gamma rays, that is, candidates for neutrino emission. Figure courtesy of A. Kappes [80].

A second kilometer-scale neutrino telescope in the Northern hemisphere is, therefore, necessary to observe the Galactic center and the largest part of the Galactic plane—or, more generally speaking, to grant full sky coverage for neutrino astronomy. The sky coverage in Galactic coordinates of IceCube and a Mediterranean-based telescope is indicated in Figure 9.

Following up the pioneering work of DUMAND, several neutrino telescope projects have been initiated in the Mediterranean in the 1990s (see above). In 2008, the construction of the ANTARES detector near the French coast off Toulon has been completed. With an instrumented volume of a percent of a cubic kilometer, ANTARES [86, 87] has about the same effective area as AMANDA and is the currently most sensitive observatory for high-energy neutrinos in the Northern hemisphere. It has demonstrated the feasibility of neutrino detection in the deep sea and has provided a wealth of technical experience and design solutions for deep-sea components.

The next step will be the construction of a multi-cubic-kilometer neutrino telescope in the Mediterranean Sea, KM3NeT. Its technical design [88] has been elaborated in

EU-funded projects (FP6 Design Study and FP7 Preparatory Phase). Major progress has been made, in particular concerning the reliability and the cost effectiveness of the design. While the original goal was to reduce the price tag for one cubic kilometer of instrumented water to \$250 M, the plan is now to construct up to 6 km^3 for this amount. A prime example for the many new technical developments is the digital optical module, which incorporates 31 3-inch photomultipliers instead of one large tube (see Figure 10). The advantages are a triplication of the photocathode area per optical module, a segmentation of the photocathode allowing for a clean identification of coincident Cherenkov photons, some directional sensitivity, and a reduction of the overall number of penetrators and connectors, which are expensive and failure prone. For all photomultiplier signals exceeding the noise level, time-over-threshold information will be digitized and time stamped by electronic modules housed inside the optical modules. Via optical fibres, this information is sent to shore, where the data stream will be filtered online for event candidates.

KM3NeT will consist of several 100 vertical structures (detection units) carrying more than 10 000 optical modules.

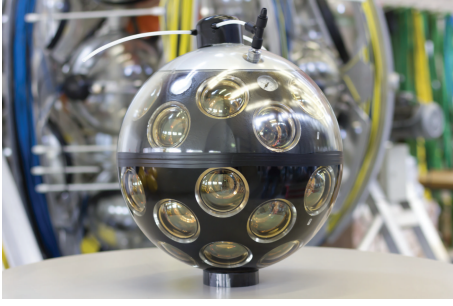


FIGURE 10: Prototype of a multi-photomultiplier optical module for KM3NeT. The module incorporates 31 3-inch photomultipliers, their high-voltage bases, and the electronic modules for signal digitization and communication to shore. Photograph by KM3NeT Collaboration.

The detection units are anchored to the sea bed with dead-weights and kept vertical by submerged buoys. The vertical distances between optical modules will be about 40 m, and the horizontal distances between detection units will be between 100 m and 180 m, depending on the outcome of ongoing optimization studies. The detector will be built in two or more large blocks, either next to each other at the same site or at different sites; candidate sites have been identified near Toulon/France (next to the ANTARES site), near Capo Passero (East of Sicily), and near Pylos (West of the Peloponnese).

Due to the drag of deep-sea currents, the detection units will deform and deviate horizontally by up to several 10 m from their nominal vertical arrangement. Acoustic triangulation, tiltmeters, and compasses will be used to monitor the position and orientation of each optical module with a precision commensurate with a timing resolution of 1 ns.

Conservative estimates of the KM3NeT sensitivity to point sources with an E^{-2} flux (see Figure 11) indicate that this detector will be more sensitive than IceCube over a large declination range. The sensitivity is also high for neutrino fluxes with cut-offs; in particular, neutrinos from the supernova remnant RX J1713-3946 should be detectable with 5σ within five years if the gamma emission from this object is of purely hadronic origin.

A first phase of KM3NeT construction is now imminent. About \$50 M of funding are available, and start of construction is expected for 2013. An option under discussion is to dedicate this first phase to a measurement of the neutrino mass hierarchy (see Section 7). A corresponding case study is in the works, and subject to its outcome, the installation of a dense array with intermodule distances much smaller than those indicated previously might be considered.

11. Conclusion: Stay Tuned

In summary, IceCube was designed for a statistically significant detection of cosmic neutrinos accompanying cosmic rays in 5 years. Here, we made the case that, based on multi-wavelength information from ground-based gamma-ray telescopes and cosmic-ray experiments, we are indeed closing

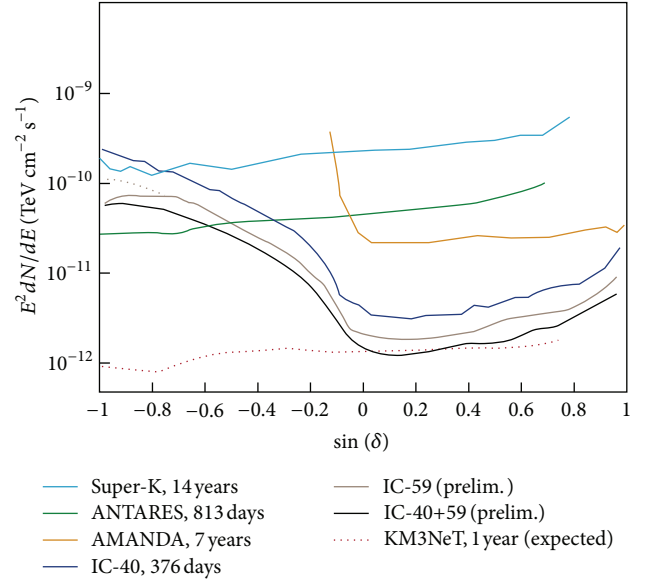


FIGURE 11: Sensitivities of running and future neutrino detectors to point source fluxes with E^{-2} spectrum as functions of the declination angle δ . Figure from [82].

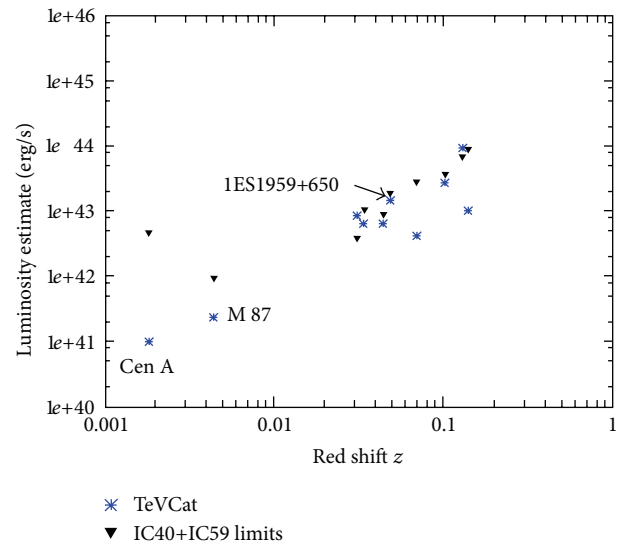


FIGURE 12: IceCube neutrino flux limits are compared with the TeV photon flux for nearby AGN. Figure courtesy of T. Gaisser [89].

in on supernova remnants, GRB (if they are the sources of cosmic rays), and GZK neutrinos. The discussion brought to the forefront the critical role of improved spectral gamma-ray data on candidate cosmic-ray accelerators. The synergy between CTA [101], IceCube, and KM3NeT as well as other next-generation neutrino detectors is likely to provide fertile ground for progress.

That, after decades of development, IceCube and KM3NeT create opportunities for discovery is illustrated by Figure 11. We recall (13) that sets the flux level of photons expected from supernova remnants if they are indeed the

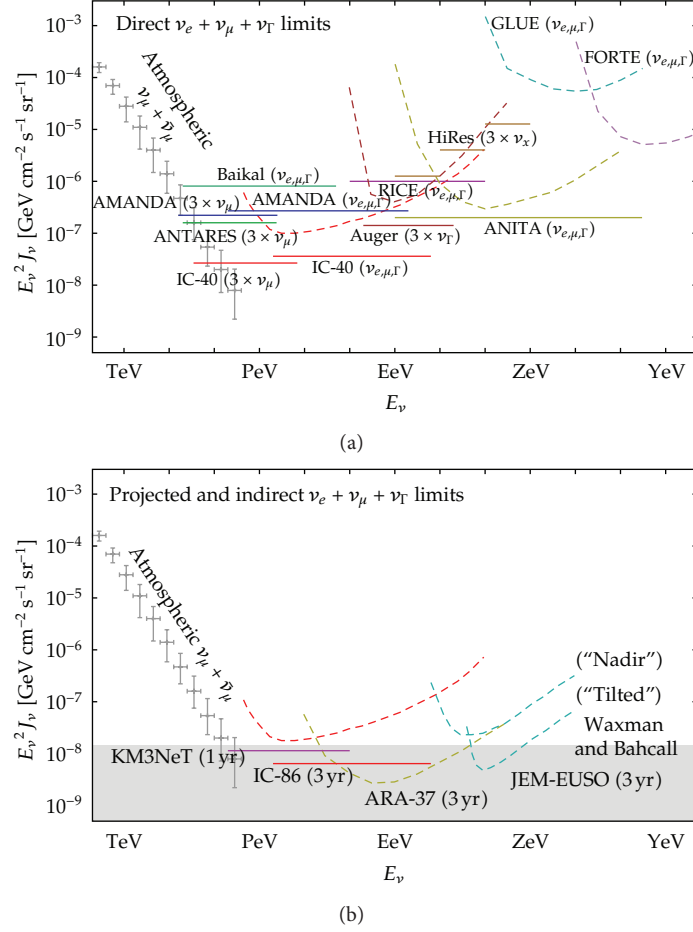


FIGURE 13: Limits on a diffuse neutrino flux from existing and, below, future experiments [16, 90–99]. Figure courtesy of M. Ahlers [100].

sources of the Galactic cosmic rays: $10^{-12} \sim 10^{-11} \text{ TeV cm}^{-2} \text{ s}^{-1}$ for a source at 1 kpc. As discussed, the Milagro experiments do observe candidate cosmic accelerators at this flux level. As can be seen from Figure 11, with a neutrino flux reduced by a factor of two, IceCube already achieved the sensitivity for possible detection with data taken during the construction phase. Subject to details of the energy spectrum and the angular extension of the sources (which becomes a problem because IceCube's resolution has improved to less than 0.5 degrees), discovery should be possible after several years, as previously argued.

The same argument can be made for extragalactic sources as already discussed in detail for the scenario where GRBs are the sources of the highest energy cosmic rays. Alternatively, Figure 12 shows the present upper limits on the neutrino flux from nearby AGN as a function of their distance. Also shown is the TeV gamma-ray emission from the same sources; except for Cen A and M 87, the muon-neutrino limits have reached the level of the TeV photon flux. This is an interesting fact as previously emphasized, one expect approximate equipartition of the cosmic-ray, gamma-ray, and neutrino fluxes from a cosmic ray accelerator. One can sum the sources shown in the figure into a diffuse flux, and the result is, after dividing by 4π , $3 \times 10^{-9} \text{ TeV cm}^{-2} \text{ s}^{-1} \text{ sr}^{-1}$,

or approximately $\sim 10^{-8} \text{ TeV cm}^{-2} \text{ s}^{-1} \text{ sr}^{-1}$ for all neutrino flavors. This is known as the Waxman-Bahcall bound; the flux is basically equal to the flux observed in extragalactic cosmic rays.

In Figure 13, we show the limits from present experiments as well as the reach of IceCube and future experiments. The benchmark flux introduced previously rises above the atmospheric neutrino background for energies exceeding 100 TeV, and an energy range entered by the completed IceCube detector after one year of operation. In fact, candidate "cosmic" neutrino events have emerged from this analysis, although their origin has not been established. We are, in any case, moving into a critical time for neutrino astronomy.

Acknowledgments

This research was supported in part by the US National Science Foundation under Grants nos. OPP-0236449 and PHY-0969061; by the US Department of Energy under Grant no. DE-FG02-95ER40896; by the University of Wisconsin Research Committee with funds granted by the Wisconsin Alumni Research Foundation and by the Alexander von Humboldt Foundation in Germany. The KM3NeT work has been supported by the EU through the KM3NeT Design

Study (Contract 011937) and the FP7 KM3NeT Preparatory Phase (Grant 212525).

References

- [1] F. Reines and C. L. Cowan Jr., "The Neutrino," *Nature*, vol. 178, no. 4531, pp. 446–449, 1956.
- [2] F. Halzen and S. R. Klein, "Astronomy and astrophysics with neutrinos," *Physics Today*, vol. 61, no. 5, pp. 29–35, 2008.
- [3] A. Roberts, "The birth of high-energy neutrino astronomy: a personal history of the DUMAND project," *Reviews of Modern Physics*, vol. 64, no. 1, pp. 259–312, 1992.
- [4] T. K. Gaisser, F. Halzen, and T. Stanev, "Particle astrophysics with high energy neutrinos," *Physics Report*, vol. 258, no. 3, pp. 173–236, 1995, Erratum, *Physics Report*, vol. 271, pp. 355–356, 1995.
- [5] J. G. Learned and K. Mannheim, "High-energy neutrino astrophysics," *Annual Review of Nuclear and Particle Science*, vol. 50, no. 1, pp. 679–749, 2000.
- [6] F. Halzen and D. Hooper, "High-energy neutrino astronomy: the cosmic ray connection," *Reports on Progress in Physics*, vol. 65, no. 7, pp. 1025–1078, 2002.
- [7] M. A. Markov, "On high-energy neutrino physics," in *Proceedings of the Annual International Conference on High Energy Physics*, E. C. G. Sudarshan, J. H. Tinlot, and A. C. Melissinos, Eds., p. 578, University of Rochester, Rochester, NY, USA, 1960.
- [8] J. Babson, B. Barish, R. Becker-Szendy et al., "Cosmic-ray muons in the deep ocean," *Physical Review D*, vol. 42, no. 11, pp. 3613–3620, 1990.
- [9] V. Balkanov, I. Belolaptikov, N. Budnev et al., "The BAIKAL neutrino project: status report," *Nuclear Physics B*, vol. 118, pp. 363–370, 2003.
- [10] G. Aggouras, E. G. Anassontzis, A. E. Ball et al., "A measurement of the cosmic-ray muon flux with a module of the NESTOR neutrino telescope," *Astroparticle Physics*, vol. 23, no. 4, pp. 377–392, 2005.
- [11] J. A. Aguilar, A. Albert, F. Ameli et al., "First results of the Instrumentation Line for the deep-sea ANTARES neutrino telescope," *Astroparticle Physics*, vol. 26, no. 4-5, pp. 314–324, 2006.
- [12] E. Migneco, "Progress and latest results from Baikal, Nestor, NEMO and KM3NeT," *Journal of Physics: Conference Series*, vol. 136, no. 2, Article ID 022048, 2008.
- [13] IceCube collaboration, "IceCube preliminary design document," 2001, <http://www.icecube.wisc.edu/science/publications/pdd/pdd.pdf>.
- [14] J. Ahrens, J. N. Bahcall, X. Bai et al., "Sensitivity of the IceCube detector to astrophysical sources of high energy muon neutrinos," *Astroparticle Physics*, vol. 20, no. 5, pp. 507–532, 2004.
- [15] J. K. Becker, "High-energy neutrinos in the context of multi-messenger astrophysics," *Physics Reports*, vol. 458, no. 4-5, pp. 173–246, 2008.
- [16] A. Achterberg, M. Ackermann, J. Adams et al., "Multiyear search for a diffuse flux of muon neutrinos with AMANDA-II," *Physical Review D*, vol. 77, no. 8, Article ID 089904, 2008, Erratum, *Physical Review D*, vol. 77, Article ID 089904, 2007.
- [17] R. Engel, D. Seckel, and T. Stanev, "Neutrinos from propagation of ultrahigh energy protons," *Physical Review D*, vol. 64, no. 9, Article ID 093010, 2001.
- [18] P. Sommers and S. Westerhoff, "Cosmic ray astronomy," *New Journal of Physics*, vol. 11, Article ID 055004, 2009.
- [19] A. M. Hillas, "Cosmic rays: recent progress and some current questions," in *Proceedings of Cosmology, Galaxy Formation and Astroparticle Physics on the Pathway to the Square Kilometre Array*, H.-R. Klockner, S. Rawlings, M. Jarvis, and A. Taylor, Eds., p. 9, ASTRON, Oxford, UK, 2008.
- [20] V. Berezhinsky, "Astroparticle physics: puzzles and discoveries," *Journal of Physics: Conference Series*, vol. 120, Article ID 012001, 2008.
- [21] R. U. Abbasi, T. Abu-Zayyad, M. Allen et al., "First observation of the Greisen-Zatsepin-Kuzmin suppression," *Physical Review Letters*, vol. 100, no. 10, Article ID 101101, 2008.
- [22] J. Abraham, P. Abreu, M. Aglietta et al., "Observation of the suppression of the flux of cosmic rays above 4×10^{19} eV," *Physical Review Letters*, vol. 101, no. 6, Article ID 061101, 2008.
- [23] H. Tokuno, T. Abu-Zayyad, R. Aida et al., "The status of the telescope array experiment," *Journal of Physics: Conference Series*, vol. 293, no. 1, Article ID 012035, 2011.
- [24] W. Rhode, K. Daum, P. Bareyre et al., "Limits on the flux of very high energy neutrinos with the Fréjus detector," *Astroparticle Physics*, vol. 4, no. 3, pp. 217–225, 1996.
- [25] W. Baade and F. Zwicky, "Remarks on super-novae and cosmic rays," *Physical Review*, vol. 46, no. 1, pp. 76–77, 1934.
- [26] Y. Butt, "Beyond the myth of the supernova-remnant origin of cosmic rays," *Nature*, vol. 460, no. 7256, pp. 701–704, 2009.
- [27] T. K. Gaisser, "Neutrino Astronomy: physics goals, detector parameters," *OECD Megascience Forum, Taormina, Italy*, <http://arxiv.org/abs/astro-ph/9707283>.
- [28] M. Ahlers, L. A. Anchordoqui, H. Goldberg, F. Halzen, A. Ringwald, and T. J. Weiler, "Neutrinos as a diagnostic of cosmic ray galactic-extragalactic transition," *Physical Review D*, vol. 72, no. 2, Article ID 023001, pp. 1–8, 2005.
- [29] E. Waxman and J. Bahcall, "High energy neutrinos from cosmological gamma-ray burst fireballs," *Physical Review Letters*, vol. 78, no. 12, pp. 2292–2295, 1997.
- [30] M. Vietri, "Ultrahigh energy neutrinos from gamma ray bursts," *Physical Review Letters*, vol. 80, no. 17, pp. 3690–3693, 1998.
- [31] M. Böttcher and C. D. Dermer, "High-energy gamma rays from ultra-high-energy cosmic-ray protons in gamma-ray bursts," *Astrophysical Journal Letters*, vol. 499, no. 2, pp. L131–L134, 1998.
- [32] S. R. Kelner, F. A. Aharonian, and V. V. Bugayov, "Energy spectra of gamma rays, electrons, and neutrinos produced at proton-proton interactions in the very high energy regime," *Physical Review D*, vol. 74, no. 3, Article ID 034018, 2006, Erratum, *Physical Review D*, vol. 79, Article ID 034018, 1995.
- [33] J. Alvarez-Muñiz and F. Halzen, "Possible high-energy neutrinos from the cosmic accelerator RX J1713.7-3946," *Astrophysical Journal Letters*, vol. 576, no. 1 II, pp. L33–L36, 2002.
- [34] J. K. Becker, F. Halzen, A. O. Murchadha, and M. Olivo, "Neutrino emission from high-energy component gamma-ray bursts," *Astrophysical Journal Letters*, vol. 721, no. 2, pp. 1891–1899, 2010.
- [35] M. C. Gonzalez-Garcia, F. Halzen, and S. Mohapatra, "Identifying Galactic PeVatrons with neutrinos," *Astroparticle Physics*, vol. 31, no. 6, pp. 437–444, 2009.
- [36] M. Ahlers, P. Mertsch, and S. Sarkar, "Cosmic ray acceleration in supernova remnants and the FERMI/PAMELA data," *Physical Review D*, vol. 80, Article ID 123017, 14 pages, 2009.
- [37] A. A. Abdu, B. Allen, D. Berley et al., "Discovery of TeV gamma-ray emission from the cygnus region of the galaxy," *Astrophysical Journal Letters*, vol. 658, no. 1 II, pp. L33–L36, 2007.

- [38] A. Djannati-Atai, E. Ona-Wilhelmi, M. Renaud et al., “H.E.S.S. Galactic plane survey unveils a milagro hotspot,” in *Proceedings of the 30th International Cosmic Ray Conference*, vol. 2, p. 1316, Merida, Mexico, 2007.
- [39] J. Albert, E. Aliu, H. Anderhub et al., “Magic observations of the unidentified γ -ray source TeV J2032+4130,” *Astrophysical Journal Letters*, vol. 675, no. 1, part 2, pp. L25–L28, 2008.
- [40] S. Gabici and F. A. Aharonian, “Searching for galactic cosmic-ray pevatrons with multi-TeV gamma rays and neutrinos,” *Astrophysical Journal Letters*, vol. 665, no. 2, pp. L131–L134, 2007.
- [41] A. A. Abdo, M. Ackermann, M. Ajello et al., “Observations of the young supernova remnant RX J1713.7-3946 with the Fermi Large Area Telescope,” *Astrophysical Journal Letters*, vol. 734, no. 1, article 28, 2011.
- [42] F. Halzen, A. Kappes, and A. Ó. Murchadha, “Prospects for identifying the sources of the Galactic cosmic rays with IceCube,” *Physical Review D*, vol. 78, no. 6, Article ID 063004, 2008.
- [43] A. Kappes, F. Halzen, and A. O. Murchadha, “Prospects of identifying the sources of the Galactic cosmic rays with IceCube,” *Nuclear Instruments and Methods in Physics Research, Section A*, vol. 602, no. 1, pp. 117–119, 2009.
- [44] D. Guetta, D. Hooper, J. Alvarez-Muñiz, F. Halzen, and E. Reuveni, “Neutrinos from individual gamma-ray bursts in the BATSE catalog,” *Astroparticle Physics*, vol. 20, no. 4, pp. 429–455, 2004.
- [45] M. Ahlers, M. C. Gonzalez-Garcia, and F. Halzen, “GRBs on probation: testing the UHE CR paradigm with IceCube,” *Astroparticle Physics*, vol. 35, no. 2, pp. 87–94, 2011.
- [46] R. Abbasi, Y. Abdou, T. Abu-Zayyad et al., “Constraints on the extremely-high energy cosmic neutrino flux with the IceCube 2008–2009 data,” *Physical Review D*, vol. 83, no. 9, Article ID 092003, 2011.
- [47] R. Abbasi, Y. Abdou, T. Abu-Zayyad et al., “Limits on neutrino emission from gamma-ray bursts with the 40 string IceCube detector,” *Physical Review Letters*, vol. 106, no. 14, Article ID 141101, 2011.
- [48] J. Abraham, P. Abreu, M. Aglietta et al., “Correlation of the highest-energy cosmic rays with nearby extragalactic objects,” *Science*, vol. 318, no. 5852, pp. 938–943, 2007.
- [49] L. A. Anchordoqui, H. Goldberg, F. Halzen, and T. J. Weiler, “Neutrino bursts from Fanaroff-Riley I radio galaxies,” *Physics Letters, Section B*, vol. 600, no. 3–4, pp. 202–207, 2004.
- [50] P. Lipari, “Problems in high-energy astrophysics,” *Proceedings of NO-VE*, <http://arxiv.org/abs/0808.0417>.
- [51] J. E. Grindlay, H. F. Helmken, R. Handburg, J. Davis, and L. R. Allen, “Evidence for the detection of gamma rays from centaurus A at E, 1011 eV,” *The Astrophysical Journal Letters*, vol. 197, p. L9, 1975.
- [52] R. W. Clay, B. R. Dawson, and R. Meyhandan, “Evidence for the detection of gamma-rays up to 150 TeV from the active galaxy Centaurus A,” *Astroparticle Physics*, vol. 2, no. 4, pp. 347–352, 1994.
- [53] W. H. Allen, I. A. Bond, E. Budding et al., “Possible observation of 100 TeV gamma rays from the active galaxy Centaurus A,” *Astroparticle Physics*, vol. 1, no. 3, pp. 269–276, 1993.
- [54] M. Punch, C. W. Akeriof, M. F. Cawley et al., “Detection of TeV photons from the active galaxy Markarian 421,” *Nature*, vol. 358, no. 6386, pp. 477–482, 1992.
- [55] S. M. Bradbury, T. Deckers, D. Petry et al., “Detection of γ -rays above 1.5 TeV from Mkn 501,” *Astronomy and Astrophysics*, vol. 320, no. 2, pp. L5–L8, 1997.
- [56] F. Aharonian, A. Akhperjanian, M. Beilicke et al., “Variations of the TeV energy spectrum at different flux levels of Mkn 421 observed with the HEGRA system of Cherenkov telescopes,” *Astronomy and Astrophysics*, vol. 393, no. 1, pp. 89–99, 2002.
- [57] D. Petry, I. H. Bond, S. M. Bradbury et al., “The TeV spectrum of H1426+428,” *The Astrophysical Journal*, vol. 580, Article ID 020750, p. 104, 2002.
- [58] F. Aharonian, A. Akhperjanian, M. Beilicke et al., “Detection of TeV gamma-rays from the BL Lac IES 1959+650 in its low states and during a major outburst in 2002,” *Astrophys*, vol. 406, Article ID 030527, pp. L9–L13, 2003.
- [59] J. Holder, I. H. Bond, P. J. Boyle et al., “Detection of TeV gamma rays from the BL Lacertae object IES 1959+650 with the Whipple 10 meter telescope,” *Astrophysical Journal Letters*, vol. 583, no. 1 II, pp. L9–L12, 2003.
- [60] F. Aharonian, A. G. Akhperjanian, G. Anton et al., “Discovery of very high energy γ -ray emission from centaurus a with H.E.S.S.,” *Astrophysical Journal Letters*, vol. 695, no. 1, pp. L40–L44, 2009.
- [61] P. Padovani and C. M. Urry, “Fanaroff-riley I galaxies as the parent population of BL lacertae objects I. X-ray constraints,” *Astrophysical Journal Letters*, vol. 356, no. 1, pp. 75–82, 1990.
- [62] M. Ahlers, L. A. Anchordoqui, M. C. Gonzalez-Garcia, F. Halzen, and S. Sarkar, “GZK neutrinos after the Fermi-LAT diffuse photon flux measurement,” *Astroparticle Physics*, vol. 34, no. 2, pp. 106–115, 2010.
- [63] A. A. Abdo, M. Ackermann, M. Ajello et al., “Spectrum of the isotropic diffuse gamma-ray emission derived from first-year fermi large area telescope data,” *Physical Review Letters*, vol. 104, no. 10, Article ID 101101, 2010.
- [64] R. Ulrich, R. Engel, S. Müller, F. Schüssler, and M. Unger, “Proton-air cross section and extensive air showers,” *Nuclear Physics B*, vol. 196, no. C, pp. 335–340, 2009.
- [65] F. Halzen, J. E. Jacobsen, and E. Zas, “Ultratransparent Antarctic ice as a supernova detector,” *Physical Review D*, vol. 53, no. 12, pp. 7359–7361, 1996.
- [66] G. Bertone, D. Hooper, and J. Silk, “Particle dark matter: evidence, candidates and constraints,” *Physics Reports*, vol. 405, no. 5–6, pp. 279–390, 2005.
- [67] B. Sadoulet, “Particle dark matter in the universe: at the brink of discovery?” *Science*, vol. 315, no. 5808, pp. 61–63, 2007.
- [68] A. Rizzo, “Search for dark matter with AMANDA and IceCube detectors,” in *Proceedings of the 7th International Heidelberg Conference on Dark Matter in Astro- and Particle Physics (Dark '09)*, H. V. Klapdor-Kleingrothaus and I. V. Krivosheina, Eds., vol. 494, World Scientific, Christchurch, New Zealand.
- [69] C. DeClercq, “Dark matter searches with AMANDA and IceCube,” in *Proceedings of PANIC*, Eilat, Israel, 2008.
- [70] J. Bagger and B. Barish, <http://www.pha.jhu.edu/~bagger/talks/HEPAP.pdf>.
- [71] L. Anchordoqui and F. Halzen, “IceHEP high energy physics at the South Pole,” *Annals of Physics*, vol. 321, no. 11, pp. 2660–2716, 2006.
- [72] J. L. Feng, A. Rajaraman, and F. Takayama, “Probing gravitational interactions of elementary particles,” *International Journal of Modern Physics D*, vol. 13, no. 10, pp. 2355–2359, 2004.
- [73] S. Pakvasa and J. W. F. Valle, “Neutrino Properties before and after KamLAND,” *Proceedings of the National Academy of Sciences, India. Section A*, vol. 70, p. 189, 2003.
- [74] O. Mena, I. Mocioiu, and S. Razzaque, “Neutrino mass hierarchy extraction using atmospheric neutrinos in ice,” *Physical Review D*, vol. 78, no. 9, Article ID 093003, 2008.

- [75] V. Barger, M. Bishai, D. Bogert et al., "Report of the US long baseline neutrino experiment study," <http://arxiv.org/abs/0705.4396>.
- [76] J. G. Learned and S. Pakvasa, "Detecting ν_τ oscillations at PeV energies," *Astroparticle Physics*, vol. 3, no. 3, pp. 267–274, 1995.
- [77] F. Halzen and D. Saltzberg, "Tau neutrino appearance with a 1000 megaparsec baseline," *Physical Review Letters*, vol. 81, no. 20, pp. 4305–4308, 1998.
- [78] E. Middell, J. McCartin, and M. D. 'Agostino, "Improved reconstruction of cascade-like events," in *Proceedings of the 31st International Cosmic Ray Conference*, vol. 5, p. 708, Lodz, Poland, 2009.
- [79] S. R. Klein, "Cascades from ν_e above 10^{20} eV," *Radiation Physics and Chemistry*, vol. 75, p. 696, 2004.
- [80] A. Kappes, "Private Communication," <http://ecap.nat.uni-erlangen.de/members/kappes/homepage>.
- [81] C. Spiering, "High energy neutrino astronomy: status and perspectives," in *4th International Meeting on High Energy Gamma-Ray Astronomy*, F. A. Aharonian, W. Hofmann, and F. Rieger, Eds., pp. 18–29, July 2008.
- [82] U. F. Katz and C. Spiering, "High-energy neutrino astrophysics: status and perspectives," *Progress in Particle and Nuclear Physics*, vol. 67, no. 3, pp. 651–704, 2012.
- [83] F. Halzen and S. R. Klein, "IceCube: an instrument for neutrino astronomy," *Review of Scientific Instruments*, vol. 81, no. 8, Article ID 081101, 2010.
- [84] F. Halzen, "Astroparticle physics with high energy neutrinos: from AMANDA to IceCube," *European Physical Journal C*, vol. 46, no. 3, pp. 669–687, 2006.
- [85] <http://www.km3net.org/>.
- [86] <http://antares.in2p3.fr/>.
- [87] ANTARES Collaboration, "ANTARES: the rst undersea neutrino telescope," *Nuclear Instruments and Methods in Physics Research Section A*, vol. 656, pp. 11–38, 2011.
- [88] KM3NeT Collaboration et al., "KM3NeT technical design report," <http://www.km3net.org/TDR/TDRKM3NeT.pdf>.
- [89] T. Gaisser, "Review of TeV gamma-ray and neutrino data of relevance to UHECR," UHECR, at CERN in February 2012, to be published in the European Physical Journal Web of Conferences.
- [90] M. Ackermann, J. Adams, J. Ahrens et al., "Search for ultra-high-energy neutrinos with AMANDA-II," *The Astrophysical Journal*, vol. 675, p. 1014, 2008.
- [91] R. Abbasi, Y. Abdou, T. Abu-Zayyad et al., "First search for extremely high energy cosmogenic neutrinos with the IceCube Neutrino Observatory," *Physical Review D*, vol. 82, Article ID 072003, 11 pages, 2010.
- [92] V. Aynutdinova, V. Balkanova, I. Belolaptikov et al., "Search for a diffuse flux of high-energy extraterrestrial neutrinos with the NT200 neutrino telescope," *Astroparticle Physics*, vol. 25, no. 2, pp. 140–150, 2006.
- [93] K. Martens, "HiRes estimates and limits for neutrino fluxes at the highest energies," in *Proceedings of the 23rd Lepton-Photon Conference*, Daegu, Republic of Korea, 2007, <http://128.84.158.119/abs/0707.4417>.
- [94] I. Kravchenko, C. Cooley, S. Hussain et al., "RICE limits on the diffuse ultrahigh energy neutrino flux," *Physical Review D*, vol. 73, no. 8, Article ID 082002, 2006.
- [95] S. W. Barwick, J. J. Beatty, D. Z. Besson et al., "Constraints on cosmic neutrino fluxes from the antarctic impulsive transient antenna experiment," *Physical Review Letters*, vol. 96, no. 17, Article ID 171101, 2006.
- [96] N. G. Lehtinen, P. W. Gorham, A. R. Jacobson, and R. A. Roussel-Dupré, "FORTE satellite constraints on ultrahigh energy cosmic particle fluxes," *Physical Review D*, vol. 69, no. 1, Article ID 013008, 2004.
- [97] P. W. Gorham, C. L. Hebert, K. M. Liewer, C. J. Naudet, D. Saltzberg, and D. Williams, "Experimental limit on the cosmic diffuse ultrahigh energy neutrino flux," *Physical Review Letters*, vol. 93, no. 4, pp. 041101–1, 2004.
- [98] L. A. Anchordoqui, J. L. Feng, H. Goldberg, and A. D. Shapere, "Neutrino bounds on astrophysical sources and new physics," *Physical Review D*, vol. 66, no. 10, Article ID 103002, 2002.
- [99] R. Abbasi, Y. Abdou, T. Abu-Zayyad et al., "Measurement of the atmospheric neutrino energy spectrum from 100 GeV to 400 TeV with IceCube," *Physical Review D*, vol. 83, no. 1, Article ID 012001, 2011.
- [100] M. Ahlers, in *Gamma-Ray Burst Symposium*, Marbella, Spain, 2012, to be published in the European Astronomical Society Publication Series.
- [101] <http://www.cta-observatory.org/>.

